

THE UNIVERSITY OF MANITOBA

THE EFFECT OF INTERFERENCE FIT ON THE DIMPLED LOADED-HOLE

FATIGUE STRENGTH OF 2024-T3 ALUMINUM ALLOY

By

Andrew P. Kuc

A Thesis  
Submitted to the Faculty of Graduate Studies  
In Partial Fulfillment of the Requirements for the Degree of  
Master of Science

Winnipeg, Manitoba

1976

"THE EFFECT OF INTERFERENCE FIT ON THE DIMPLED LOADED-HOLE  
FATIGUE STRENGTH OF 2024-T3 ALUMINUM ALLOY"

by

ANDREW P. KUC

A dissertation submitted to the Faculty of Graduate Studies of  
the University of Manitoba in partial fulfillment of the requirements  
of the degree of

MASTER OF SCIENCE

© 1976

Permission has been granted to the LIBRARY OF THE UNIVER-  
SITY OF MANITOBA to lend or sell copies of this dissertation, to  
the NATIONAL LIBRARY OF CANADA to microfilm this  
dissertation and to lend or sell copies of the film, and UNIVERSITY  
MICROFILMS to publish an abstract of this dissertation.

The author reserves other publication rights, and neither the  
dissertation nor extensive extracts from it may be printed or other-  
wise reproduced without the author's written permission.

## ABSTRACT

The effect of interference fit on the fatigue strength of loaded holes is well known. Recently, a new technique has been developed for increasing this strength in thin sheet material. Briefly, the technique consists of dimpling the material centering about the region where the hole is to be made thus introducing tensile plastic strain. The dimple is then flattened and the hole drilled leaving the region around the hole under residual compressive stress.

Experiments were carried out to obtain the combined effect of interference and dimpling in loaded-hole fatigue applications.

In zero-to-tension fatigue tests on nominally 0.063 in. thick 2024-T3 aluminum alloy specimens, optimum tapered-pin interference and dimpling combined gave a fatigue strength improvement factor of 4.0 while the dimpling technique increased the fatigue strength by a factor of 2.85 all at  $10^6$  cycles to failure.

ACKNOWLEDGMENTS

The author wishes to extend special thanks to Dr. John Shewchuk, thesis advisor, for his invaluable guidance and assistance. Gratitude is also extended to Don Mardis of the Metallurgy Group of the Department of Mechanical Engineering, to Oscar Tonn, chief technician of the Department, and to Les Wilkins and Rod Sharpe, who are machine shop supervisor and associate respectively for the Department, for freely making available information and expertise. The assistance of Horst Weiss, Ken Tarte, and Prabir Mitra of the Drafting Group and of Mrs. Rita Hanley of the Department in the preparation of this thesis is also gratefully acknowledged by the author.

The research was supported by the National Research Council of Canada through operating grant A4131 to Dr. John Shewchuk. The author wishes to express his gratitude for the financial assistance.

Special thanks are also due to my mother and father.

TABLE OF CONTENTS

	<u>Page</u>
ABSTRACT . . . . .	i
ACKNOWLEDGMENTS . . . . .	ii
TABLE OF CONTENTS . . . . .	iii
LIST OF TABLES . . . . .	v
LIST OF FIGURES . . . . .	vi
NOMENCLATURE . . . . .	ix
CHAPTER 1 INTRODUCTION . . . . .	1
1.1 Introduction . . . . .	1
1.2 Scope of the Present Research . . . . .	3
CHAPTER 2 REVIEW OF LITERATURE ON FATIGUE STRENGTHENING OF LOADED HOLES . . . . .	4
2.1 Introduction . . . . .	4
2.2 The Interference-Fit Method . . . . .	4
2.3 The Dimpling Method . . . . .	17
2.4 Closure . . . . .	18
CHAPTER 3 THE DIMPLING-INTERFERENCE METHOD . . . . .	20
3.1 Introduction . . . . .	20
3.2 The Dimpling Mechanism . . . . .	20
3.3 The Interference Mechanism . . . . .	23
3.4 The Dimpling-Interference Mechanism . . . . .	26
3.5 Closure . . . . .	29

Page

CHAPTER 4	EXPERIMENTAL STUDY . . . . .	30
4.1	Introduction . . . . .	30
4.2	Test Program . . . . .	30
4.3	Test Details . . . . .	31
4.3.1	Material and Specimens . . . . .	31
4.3.2	Specimen Preparation . . . . .	31
4.3.3	Interference Technique . . . . .	35
4.3.4	Test Procedure . . . . .	35
4.4	Test Results . . . . .	38
CHAPTER 5	ANALYSIS OF RESULTS . . . . .	43
5.1	Introduction . . . . .	43
5.2	Dimpling . . . . .	43
5.3	Interference Technique . . . . .	44
5.4	Interference Optimization . . . . .	49
5.5	Dimpling With Optimum Interference . . . . .	53
5.6	Interference Versus Crack Location . . . . .	54
5.7	Prediction of Fatigue Strength and Life . . . . .	54
CHAPTER 6	SUMMARY AND CONCLUSIONS . . . . .	68
6.1	Summary . . . . .	68
6.2	Conclusions . . . . .	68
6.3	Suggestions for Further Study . . . . .	69
BIBLIOGRAPHY	. . . . .	70

LIST OF TABLES

<u>Table</u>		<u>Page</u>
2.1	Alternating Stresses ( $\pm$ ksi) in Aluminum Alloy Lugs Failing in $10^6$ Cycles, Showing the Effect of Interference at Various Mean Stresses (7) . . . . .	12
2.2	Strength or Life Improvement Factors Established With the Interference and Dimpling Techniques . . . . .	19
4.1	Chemical and Mechanical Properties of 2024-T3 Alclad Aluminum Alloy Sheet . . . . .	32
4.2	Results of Fatigue Tests on Plain Specimens With and Without Pin Interference . . . . .	42
5.1	Calculated $K_f$ Values for Loaded-Hole Specimens . . . . .	50
5.2	Interference Hole Boundary Hoop Stresses for Loaded-Hole Specimens . . . . .	51
5.3	Comparison of Present Investigation to Low (9), Hartman and Jacobs (8), and Smith (10) . . . . .	52
5.4	Comparison of Predicted and Actual Fatigue Lives . . . . .	66

LIST OF FIGURES

<u>Figure</u>	<u>Page</u>
2.1 Approximate Distribution of Hoop Tensile Stress Around the Hole Boundary ( $d/D = 0.375$ ). Stress Conditions Apply to Aluminum Lugs and Steel Pins. Photoelastic Analysis (1) . . . . .	6
2.2 Effect of Interference on Maximum Shear Stress on Horizontal Section of Lug (1) . . . . .	7
2.3 Distribution of Shear Stress Around the Hole Boundary ( $d/D = 0.375$ ), (1) . . . . .	8
2.4 Schematic Diagram of Minimum Section, Hole Boundary Hoop Stress Versus Applied Pin Load. Photoelastic Analysis (2) . . . . .	10
2.5 Effect of Interference on Fatigue Strength of Aluminum Alloy Lugs (8). Material: 24S-T Alclad Sheet. Dimensions: $d = 0.394$ , $D = 1.18$ inch . . . . .	13
2.6 Effect of Interference on Fatigue Strength of Aluminum Alloy Lugs (8). All Conditions as in Figure 2.5 Except $d = 0.236$ inch. . . . .	13
2.7 Effect of Interference on Fatigue Strength of Aluminum Alloy Lugs (9). Material: B.S. L65 . . . . .	15
2.8 Effect of Taper-Pin Interference in Fatigue Life of Small Lugs (11). Material: 7075-T6 Aluminum Alloy . . .	16



<u>Figure</u>	<u>Page</u>
3.1 Concentric Dimpling . . . . .	21
3.2 Optimum Dimpling Residual Stresses (14). . . . .	22
3.3 Dimpling Mechanism . . . . .	24
3.4 Interference Mechanism . . . . .	25
3.5 Goodman-Type Fatigue-Strength Diagram Constructed from Unnotched Data for 2024-T3 Alclad Aluminum Alloy Sheet (15) . . . . .	27
3.6 Dimpling-Interference Mechanism . . . . .	28
4.1 Test Specimen . . . . .	33
4.2 Dimpling - Indentation . . . . .	34
4.3 Dimpling - First Stage Flattening . . . . .	34
4.4 Dimpling - Second Stage Flattening . . . . .	34
4.5 Hole Preparation - Reaming . . . . .	36
4.6 Interference Technique . . . . .	37
4.7 Loading Arrangement . . . . .	39
4.8 Dimpled Specimen Interference Optimization Results . . . . .	40
4.9 Fatigue Test Results . . . . .	41
5.1 Theoretical Stress Concentration Factors, $K_t$ , for Loaded Lugs with Small Clearance Between Hole and Pin . . . . .	47
5.2 Neuber Constants for Steel and Aluminum . . . . .	48
5.3 Interference Versus Crack Location . . . . .	55
5.4 Graphical Method of Fatigue Strength Prediction . . . . .	57
5.5 Variation of the Present Experimental Fatigue Strength Reduction Factor, $K_f$ , With Life . . . . .	59

<u>Figure</u>		<u>Page</u>
5.6	'Notched' Failure Lines for the Present Investigation . . . . .	60
5.7	'Notched Failure Line for $10^6$ Cycles to Failure (7) . . . . .	61
5.8	Interference Hoop Stress Profile Over the Minimum Net Section for the Present Investigation . . . . .	63
5.9	Variation of $S_a$ With Interference for a Pin-Loaded Hole Subjected to Zero-to-Tension Loading . . . . .	64

NOMENCLATURE

- $P$  - applied pin load  
 $d$  - nominal pin and hole diameter  
 $D$  - width of lug  
 $H$  - head height of lug on loaded side of hole  
 $t$  - thickness of lug  
 $\delta$  - initial difference between mating pin and hole diameters  
 $S_m$  - mean stress  
 $S_a$  - alternating stress  
 $S_{NET}$  - net stress  
 $S_{MIN}$  - minimum stress  
 $S_{MAX}$  - maximum stress  
 $S_{NOM}$  - nominal applied stress over the minimum net section  
 $N$  - cycles to failure  
 $K_f$  - fatigue strength reduction factor  
 $K_t$  - theoretical stress concentration factor  
 $a$  - a material constant representing the half length of a fictitious "building block" or "equivalent grain" of the material  
 $r$  - hole radius  
 $S_{INT}$  - initial interference hole boundary hoop stress  
 $P_a$  - alternating pin load  
 $P_m$  - mean pin load  
 $S_{a,NOM}$  - nominal alternating stress over the minimum net section

## CHAPTER 1

### INTRODUCTION

#### 1.1 Introduction

Since the introduction of machinery, mechanical elements, subjected to fluctuating loads, have been a victim of a mode of failure characterized as fatigue. Failure is abrupt and may occur in both a ductile and a brittle metal and at stresses substantially below the yield point of the material. Small wonder that investigators have spent over a century in attempting to understand the nature of and find the remedy to fatigue.

Metallurgical research conducted on the microscopic level has led to the acceptance of two failure mechanisms based on the popular Dislocation Theory. They are the nucleation of microcracks through the process of slip and the propagation of microcracks by the rupturing of atomic bonds at the crack tips through the action of applied tensile stresses normal to the crack plane. Numerous fatigue tests, on the other hand, have provided a storehouse of data on the macroscopic fatigue properties of particular materials. Surface finish, type of loading, nature of load fluctuation, grain size and orientation, size of part, and atmospheric environment are but a few of the many variables found to affect these properties. Yet, despite the vast amount of knowledge and empirical data available, the complexity of fatigue has permitted mechanical designers to only crudely approximate the fatigue strengths or service lives of even simple components.

In fatigue, damage begins in the portions of the material which cannot support the applied stresses experienced therein. Fatigue is therefore a localized phenomenon. Consequently, microcracks tend to form at points of stress concentration. On the microscopic level, these may be represented by grain boundaries, voids, or other discords in atomic matrix. On the macroscopic level, holes, fillets, grooves, threads, seams, keyways or any one of a number of discontinuities required by design in the shape of a part are almost invariably the origins. Once microcracks have reduced a loaded cross section sufficiently, the remaining undamaged material in the section may suffer a brittle fracture.

At one time, if a part failed in fatigue it was simply replaced by a larger, stronger one. If this proved inconvenient, the design was altered. In engineering, and particularly where size and weight are crucial factors, it is desirable for a machine element to display a high fatigue and/or static strength to weight ratio. To accomplish the former in the presence of stress concentrations, beneficial residual compressive stresses are generally induced in the critically stressed material about the concentrations. Applied loads are then more evenly distributed over the cross sections in question, leading to higher joint efficiencies.

The improvement of fatigue strengths or the extension of service lives is still the continuing concern of much research. One is constantly striving to provide sounder guarantees on the performance of components especially when human lives may be involved. This thesis highlights a particular sample of such research.

## 1.2 Scope of the Present Research

The present experimental investigation proposes and examines the effectiveness of a new method for increasing the fatigue strength of loaded-hole connections in sheet material. The method entails combining two previously established techniques, dimpling and interference. Dimpling induces beneficial residual compressive stresses around concentrations and interference operates to reduce harmful stress fluctuations over the critical cross section of the loaded sheet material.

## CHAPTER 2

REVIEW OF LITERATURE ON FATIGUE  
STRENGTHENING OF LOADED HOLES2.1 Introduction

A major concern of mechanical designers is the harmful effect of stress concentrators on the fatigue life of components. Both an interference fit and the new technique termed dimpling have individually been proven successful in improving the fatigue strength of loaded holes by reducing the effect of the stress concentrator. A representative survey of published research involving the use of interference fits and dimpling follows.

2.2 The Interference-Fit Method

Interference will be defined throughout the entire thesis as:  
 $\{d(\text{pin}) - d(\text{hole})\}/d(\text{hole})$ .

An interference fit, created by the insertion of an oversized pin into a given size hole, has been studied by stress analysts and fatigue researchers alike.

Jessop, Snell and Holister (1) performed a photoelastic investigation on the variation of the hoop tensile stresses and the shear stresses in a plate around a hole boundary with pin load for the cases of a push fit and interference fits between the pin and the plate. With interference, all the mean stresses were enhanced, but the majority of the alternating

stresses were considerably reduced. Figure 2.1 illustrates the approximate distribution of hoop stress around the hole boundary as found by the above investigators for the case of a steel pin in an aluminum alloy lug. The maximum hoop tensile stress occurred on the minimum transverse section for both a push-fit pin and for the two degrees of interference. In addition, at a maximum pin load of  $32 \times 10^3$  LB./IN.<sup>2</sup>, the resultant maximum hoop tensile stress was reduced by approximately 20 and 34 percent with interferences of 0.003 and 0.006 inch per inch hole diameter respectively. The maximum shear stress on the horizontal diameter versus pin load is shown in Figure 2.2. The interference reduced the rate of increase of stress at low loads, but gave the normal rate for higher loads, as would be obtained for the push-fit case. Figure 2.3 presents the distribution of shear stress found around the hole boundary. The maximum shear stress for the push-fit case occurred about  $30^\circ$  from the horizontal diameter on the loaded side of the hole but this maximum was displaced towards the horizontal diameter as the interference was increased.

Ligenza (2) also employed photoelasticity to study the variation, with load, of the maximum hoop tensile stress on the hole boundary of the horizontal diameter in a pin-loaded, semicircular-ended lug for various amounts of interference furnished by interference-fit liners. The variation found for an interference fit bore a resemblance to the one found by Jessop, Snell and Holister. That is, the applied load changed the maximum hoop tensile stress only slightly at lower load levels and at a slight rate of increase at intermediate loads, until, at a critical level,



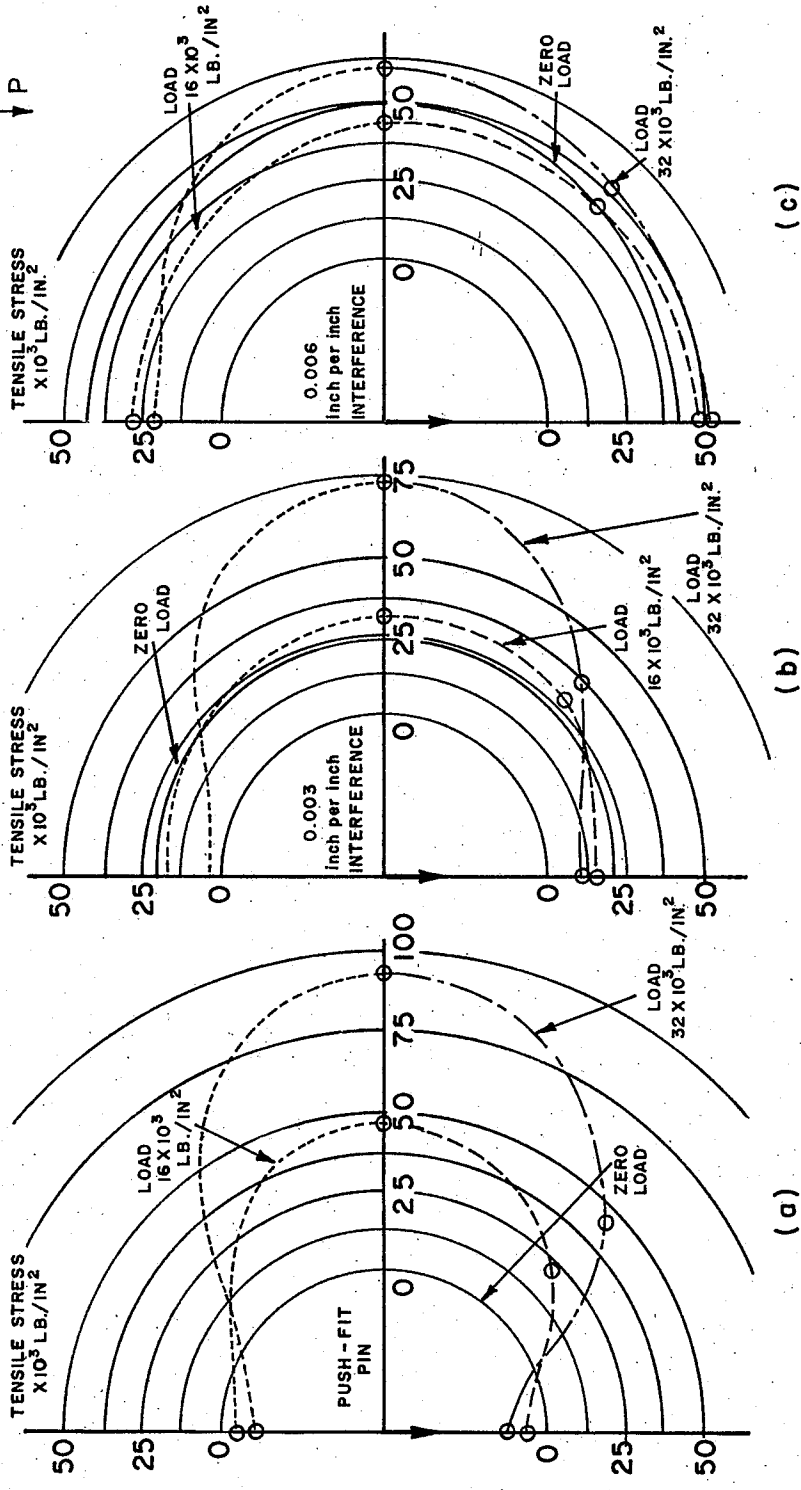
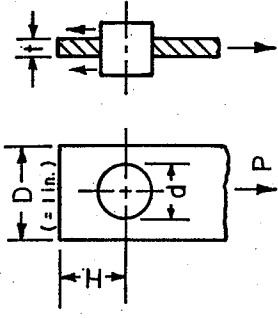


Figure 2.1 Approximate Distribution of Hoop Tensile Stress Around the Hole Boundary ( $d/D = 0.375$ ). Stress Conditions Apply to Aluminum Alloy Lugs and Steel Pins. Photoelastic Analysis (1).

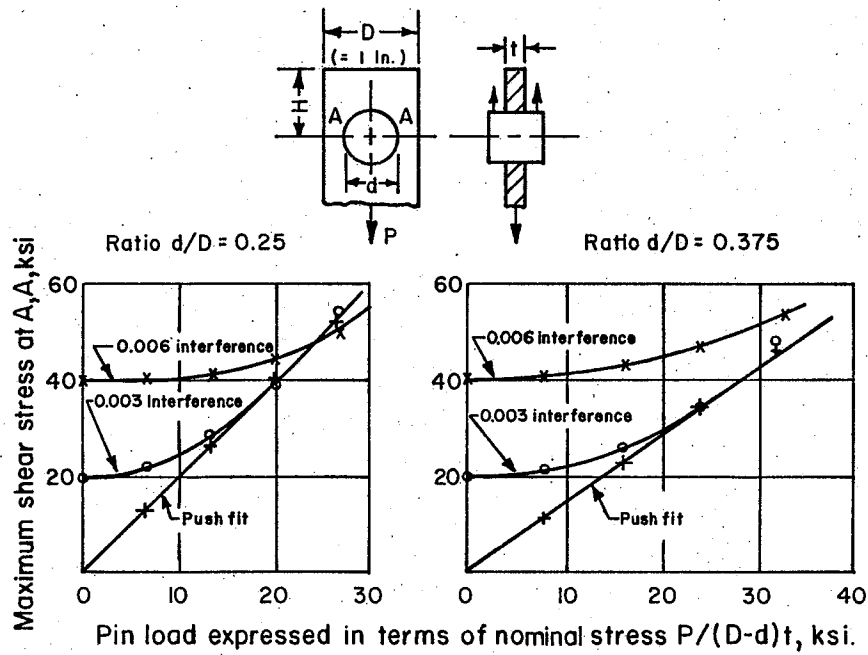


Figure 2.2 Effect of Interference on Maximum Shear Stress on Horizontal Section of Lug (1)

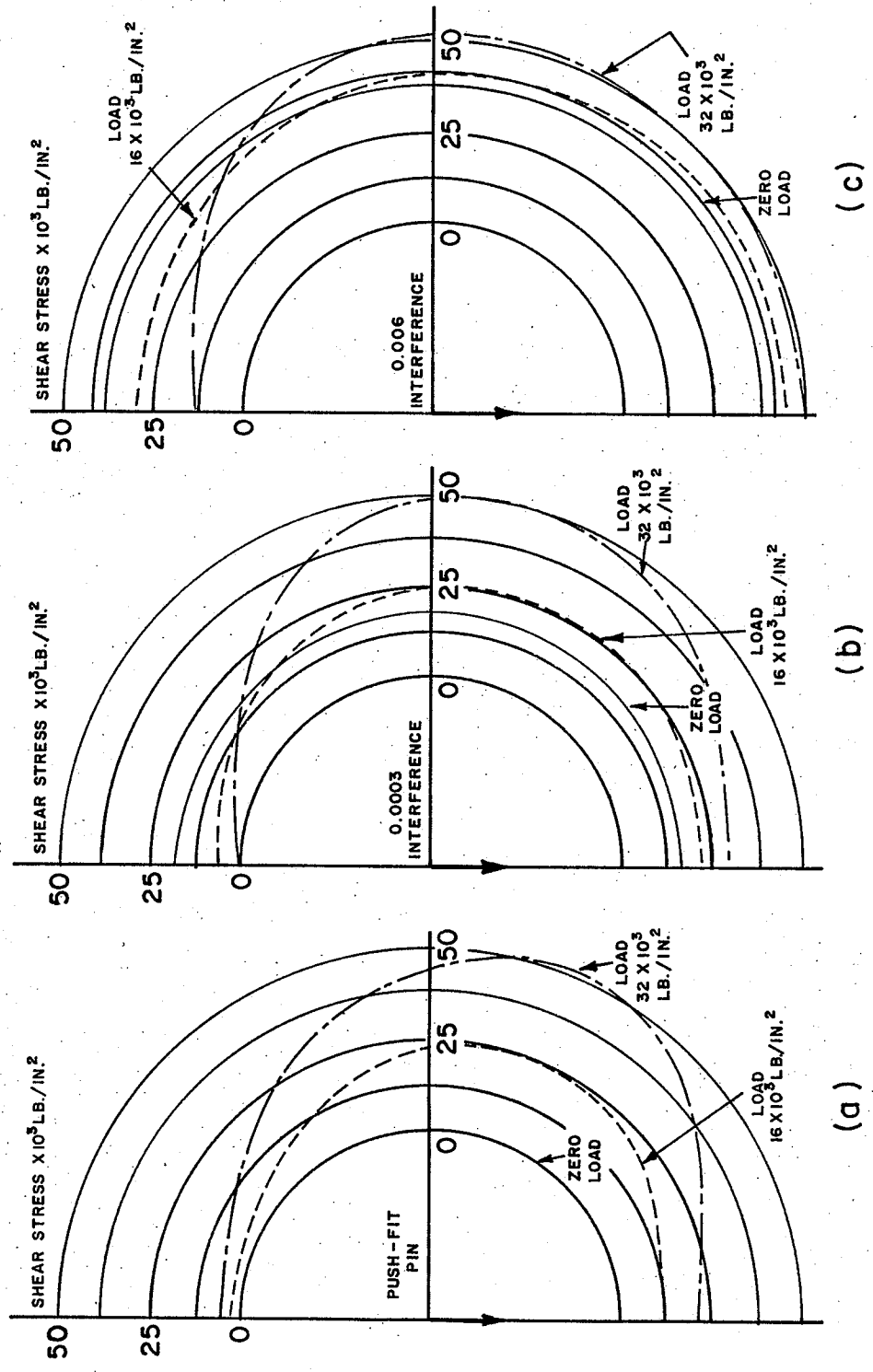


Figure 2.3 Distribution of Shear Stress Around the Hole Boundary ( $d/D = 0.375$ ), (1)

the stress became proportional to load, as shown in Figure 2.4. Based upon the measurements of the variation of maximum hoop tensile stress with load at various levels of interference and for several lug configurations, Ligenza showed that interference fits could be used to combat fatigue within pin-loaded lugs by reducing cyclic-stress levels at the critical regions and that an optimum level of interference exists with each applied load for each lug-liner configuration.

Lambert and Brailey (3), with the use of photoelasticity, discovered that with an initial interference fit between pin and plate, the increase in maximum shear stress for a given increase in load increased with increasing load but that the stress-load relationship showed a distinct discontinuity. The load at which this discontinuity occurred was dependent upon both the initial interference and the coefficient of friction between the pin and the plate. A high coefficient of friction coupled with an initial interference fit effectually reduced the shear stress concentration factor.

In an early work on the effect of an interference fit on fatigue life, Fisher and Winkworth (4) showed that little improvement in fatigue life was obtained with straight-shank fasteners for interferences within shop tolerances. Later, (5), they discovered that for interferences exceeding 0.0043 inch per inch of diameter, an increase from about 300,000 cycles for a small clearance to non-failure in 10,000,000 cycles was usually obtained in B.S. L65 Al-Cu alloy lugs of the square-ended type subjected to fluctuating nominal tensile stresses on the minimum section

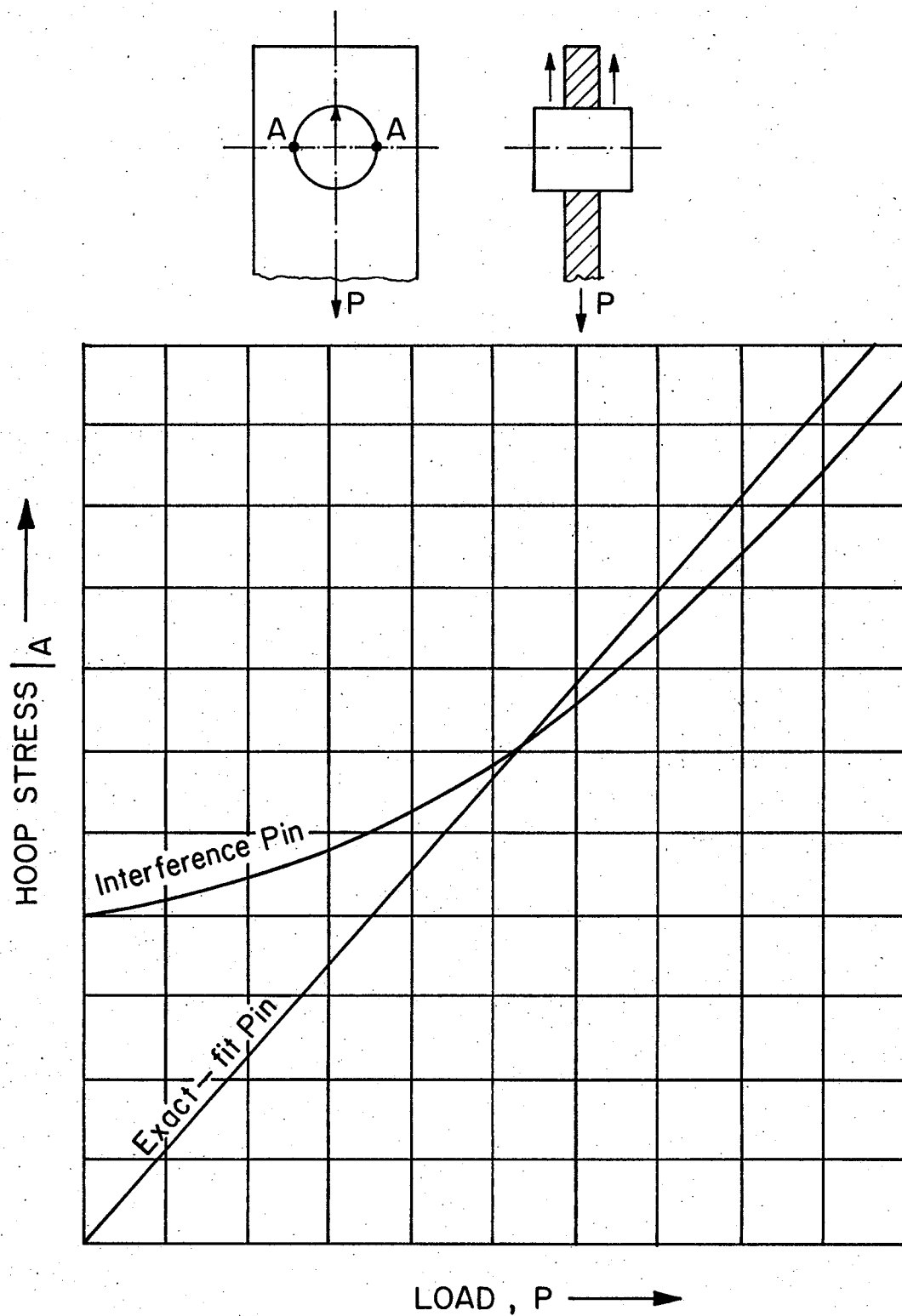


Figure 2.4 Schematic Diagram of Minimum Section, Hole Boundary Hoop Stress Versus Applied Pin Load. Photoelastic Analysis (2)

of  $13.4 \pm 4$  ksi. This improvement was also obtained for a mild steel bush-pin combination when the interference exceeded 0.0032 inch per inch.

Schijve, Broek and Jacobs (6) also found that an interference of 0.4 percent of hole diameter was required to show a definite fatigue-life improvement in aluminum alloy lugs.

Fisher and Yoemans (7) studied the effect of interference at three mean stress levels for lugs in the Al-Cu alloy B.S. L65 and the Al-Zn-Mg alloy DTD 363. The results, entered in Table 2.1, show that a considerable improvement in fatigue strength was achieved by increasing the interference from 0.001 to 0.0043 inch per inch, the greatest increases being obtained when the mean stress was 11.2 ksi.

Conducting zero-to-tension fatigue tests, Hartman and Jacobs (8) examined the effect of interference and clearance, with life, on the fatigue strength of 24S-T Al-Cu alloy lugs. The S-N curves found are displayed in Figures 2.5 and 2.6. The maximum interference values of 0.004 and 0.0067 inch per inch tested provided fatigue strength improvement factors of 2.2 and 2.0 in comparison to clearance at  $10^6$  cycles to failure for the larger and smaller hole diameter-to-width of lug ratios respectively. Further, in each case, the beneficial effect of interference continually decreased as the life decreased.

From performing direct stress, tension-tension fatigue tests on square-ended lugs made from the aluminum-copper alloy B.S. L65, Low (9) observed that the fatigue strength progressively increased with increase in interference, up to an upper limit represented approximately by the

TABLE 2.1

Alternating Stresses ( $\pm$  ksi) in Aluminum Alloy Lugs  
 Failing in  $10^6$  Cycles, Showing the Effect of Interference  
 at Various Mean Stresses (7)

Row	Interference (inch/inch)	Al-Cu alloy B.S. L65 with mean stress (ksi) of			Al-Zn-Mg alloy DTD 363 with mean stress (ksi) of	
		0	11.2	16.8	11.2	16.8
A	0.001	<u>+9.4</u>	3.15	2.5	3.5	2.9
B	0.0043	<u>+13.3</u>	7.6	3.4	7.2	4.8
Ratio B/A		1.4	2.4	1.35	2.1	1.65

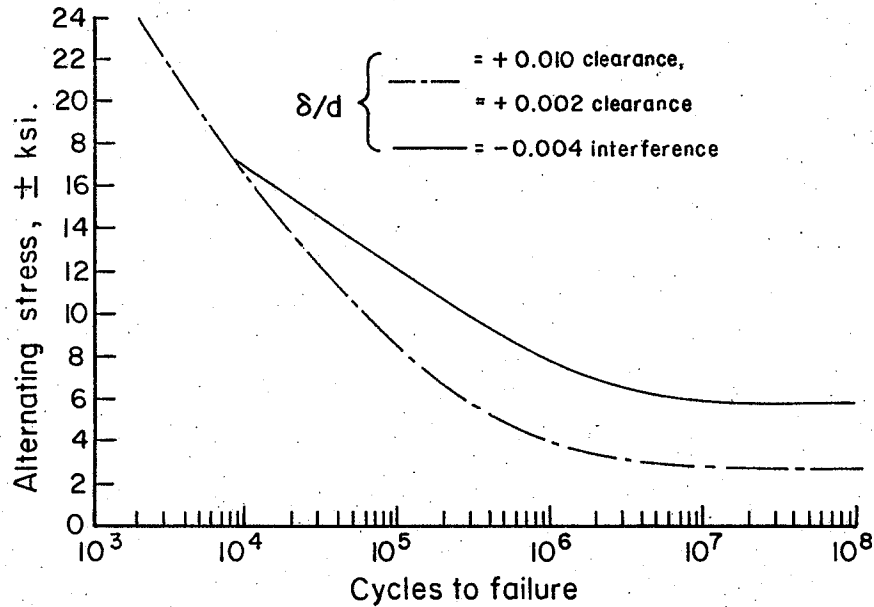


Figure 2.5 Effect of Interference on Fatigue Strength of Aluminum Alloy Lugs (8). Material: 24S-T Alclad Sheet. Dimensions:  $d = 0.394$ ,  $D = 1.18$  inch

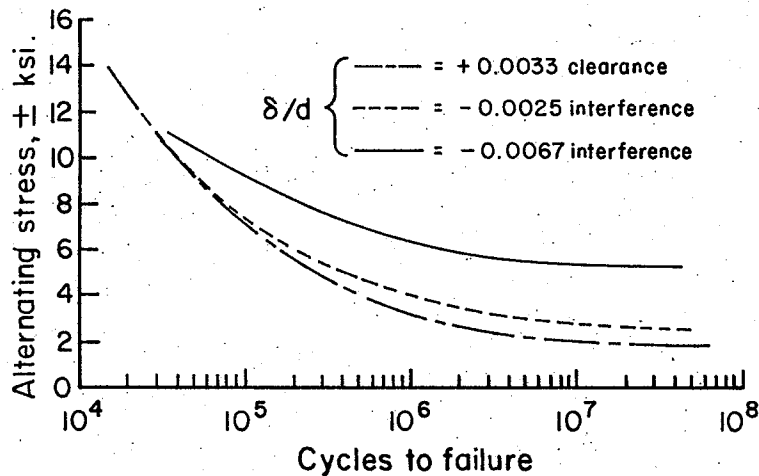


Figure 2.6 Effect of Interference on Fatigue Strength of Aluminum Lugs (8). All Conditions as in Figure 2.5 except  $d = 0.236$  inch



high interference of 0.007 inch per inch with which the load-carrying capacity for a service life of  $10^6$  cycles was increased by about 300 percent. In addition, with reference to Figure 2.7, the author suggested that the best interference may vary with the design life (or loading) of the joint.

Smith (10) also arrived at the conclusion that one and only one amount of interference is optimum for a given loading of a component. Zero-to-tension fatigue tests on the effect of pressed-in bushings of hardened steel on the fatigue life of semicircular-ended lugs of 7075-T6 aluminum alloy indicated an optimum interference of 0.006 inch per inch of hole diameter for which a fatigue life of over a million cycles was achieved as compared to 34,500 cycles with no interference and for the same loading. The average fatigue lives with interference values of 0.004 and 0.008 inch per inch were significantly greater than the average obtained with no interference but were less than the average achieved using an interference of 0.006 inch per inch. Smith (11) added further support to the concept of an optimum interference for a given loading of a component by developing the life versus interference curve in Figure 2.8 for small 0.10-inch-thick lugs of 7075-T6 aluminum alloy tested at approximately  $6.0 \pm 6.0$  ksi gross area stress and using taper pins to provide known amounts of interference.

Mittenbergs and Beall (12) showed that with increasing interference, the fatigue strength of SAE 4340 steel, pin-loaded lugs subjected to a combined loading consisting of a steady tension component and an

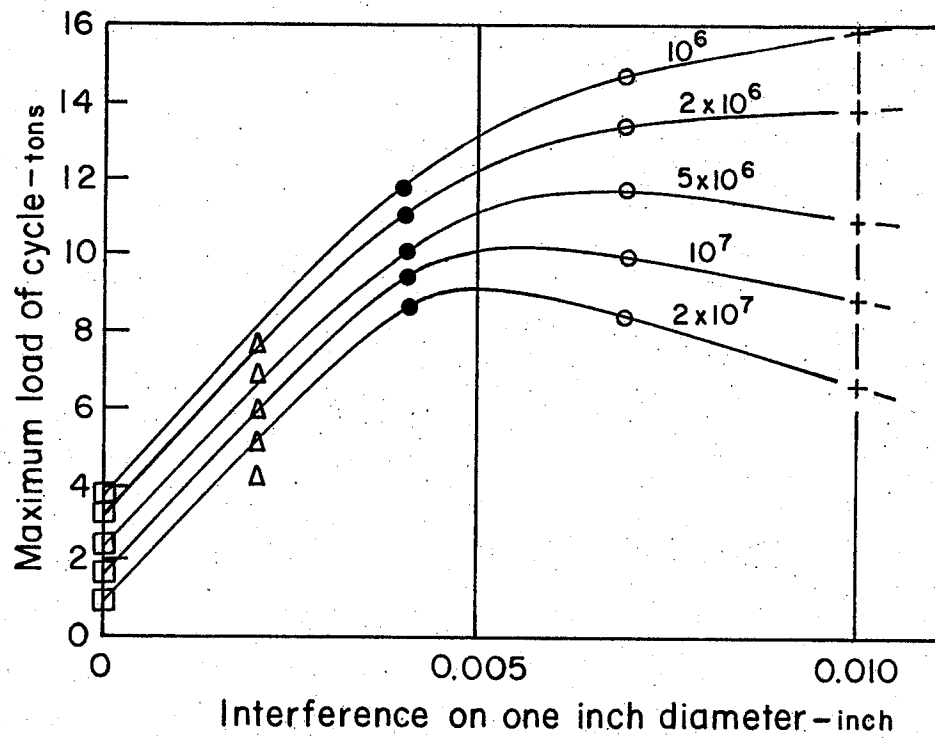


Figure 2.7 Effect of Interference on Fatigue Strength of Aluminum Alloy Lugs (9)

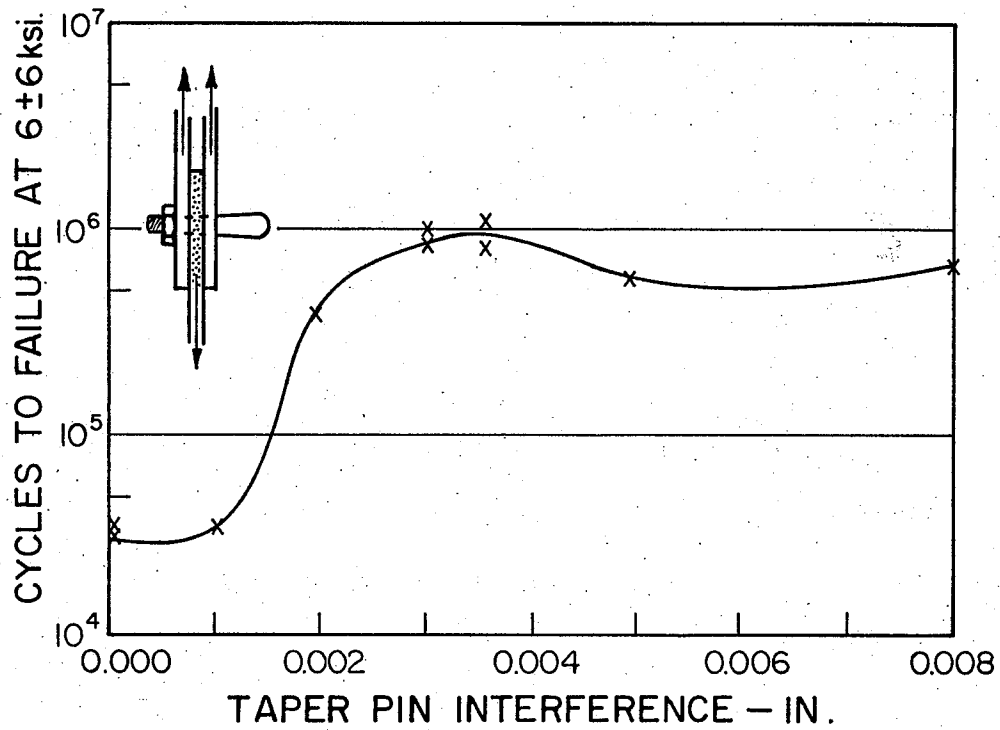


Figure 2.8 Effect of Taper-Pin Interference in Fatigue Life of Small Lugs (11). Material: 7075-T6 Aluminum Alloy

alternating reversed cantilever-type bending moment was continually improved. Pin interferences of 0.0005, 0.002, and 0.003 inch per inch of diameter were tested. Compared to a pin interference of 0.0005 inch per inch, an interference of 0.002 inch per inch increased the moment-carrying capacity by about 90 percent and that of 0.003 inch per inch by about 150 percent. All failures originated at the pinhole interface. Fretting was present in the locations of failure origins. The fretted areas, however, generally decreased with increasing pin interference.

Using small-pinned connections made from FV 520B alloy steel, White (13) found that, in pulsating tension tests, the fatigue strength increased linearly with interference for the range of pin-interference tested. At a maximum pin interference of 0.004 inch per inch an improvement in strength, expressed as a ratio of the strength of the joint with that employing an exact-fit pin, of 2.0 was acquired at a life of  $10^6$  cycles. The exact-fit specimens failed on the horizontal center-line where fretting occurred and the stress was the highest. In specimens with interference-fit pins, both fretting and cracking were displaced from the horizontal center-line in the direction of the unloaded side of the hole, the displacement increasing with increasing interference.

### 2.3 The Dimpling Method

Recently, Shewchuk and Roberts (14) have shown in zero-to-tension fatigue tests that considerable improvement in the fatigue strength of loaded holes in sheet material is possible as a result of dimpling, a

technique of inducing residual compressive stresses in a plate material around a hole prior to loading. A fatigue strength improvement factor of nearly 3.0 for  $10^6$  cycles to failure was obtained based on the median lives of nominally 0.050-inch-thick 2024-T3 alclad aluminum alloy specimens.

Employing the dimpling process, Shewchuk (15) later discovered that a fatigue strength reduction factor of 2.2 for an unloaded hole in nominally 0.050-inch-thick 2024-T3 alclad aluminum alloy specimens was reduced by approximately 36 percent at  $10^6$  cycles to failure in zero-to-tension fatigue tests.

#### 2.4 Closure

The end effects of interference fits and dimpling on the fatigue strength of loaded holes have been presented. Table 2.2 summarizes the fatigue strength or life improvements found by the aforesaid investigators. Differences in loading, design and material of specimens among the investigations, however, make a direct comparison of results impossible. In addition, techniques for fatigue strength improvement generally increase in effectiveness with increasing life. Thus the strength improvement factors for (12) and (13) would be less than 2.5 and 2.0 respectively at  $10^6$  cycles to failure. In the next chapter, the ruling mechanism(s) of each technique will be discussed.

TABLE 2.2

Strength or Life Improvement Factors Established with  
the Interference and Dimpling Techniques

Technique	Investigator	Strength improvement factor at given life	Life improvement factor
Interference	Fisher & Winkworth (5)		33.3
	Fisher & Yeomans (7)	1.35 - 2.4 at $10^6$	
	Hartman & Jacobs (8)	2.0 - 2.2 at $10^6$	
	Low (9)	4.0 at $10^6$	
	Smith (10)		31.6
	Smith (11)		28.0
	Mittenbergs & Beall (12)	2.5 at $10^7$	
	White (13)	2.0 at $10^8$	
Dimpling	Shewchuk & Roberts (14)	2.92 at $10^6$	
	Shewchuk (15)	1.64 at $10^6$	

## CHAPTER 3

## THE DIMPLING-INTERFERENCE METHOD

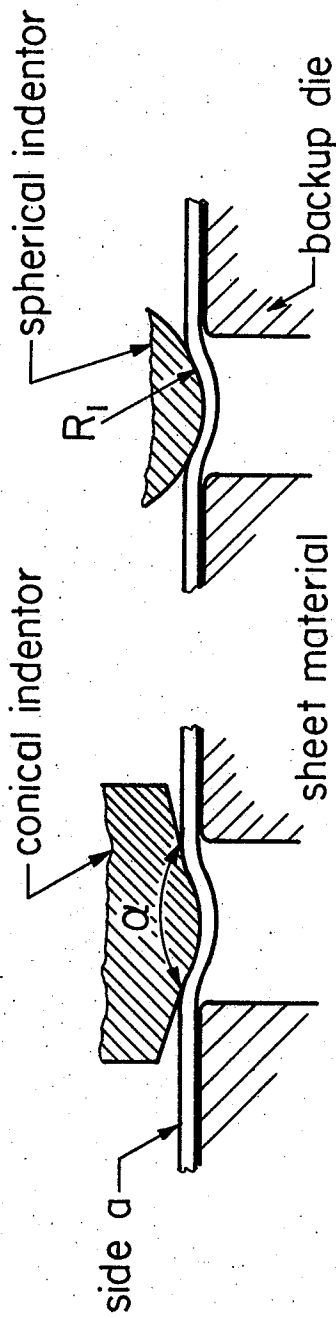
3.1 Introduction

The fatigue life of a given component is governed essentially by the mean and alternating stresses that it experiences under the action of applied loads, and by the nature of fretting which occurs. For metals, mean and alternating stresses have a more adverse effect on the life as each is intensified. Damage induced by fretting is dependent upon both the normal pressure and the relative slip at points of contact between components. By appropriately controlling one or more of these factors, an enhanced fatigue life should result.

3.2 The Dimpling Mechanism

Dimpling is a recent technique of introducing residual compressive stresses in a plate material around a hole prior to loading. Briefly, the technique, as illustrated in Figure 3.1, consists of dimpling the material centering about the region where the hole is to be made, thus introducing tensile plastic strain. The dimple is then flattened and the hole drilled leaving the region around the hole under residual compressive stresses. Employing the X-ray diffraction technique, Shewchuk and Roberts (14) found the stress distributions of Figure 3.2 to be associated with the optimum indenter-die combination. Note the fairly broad peaks for the hoop stresses except very near to the hole boundary where it is

# DIMPLING



# FLATTENING

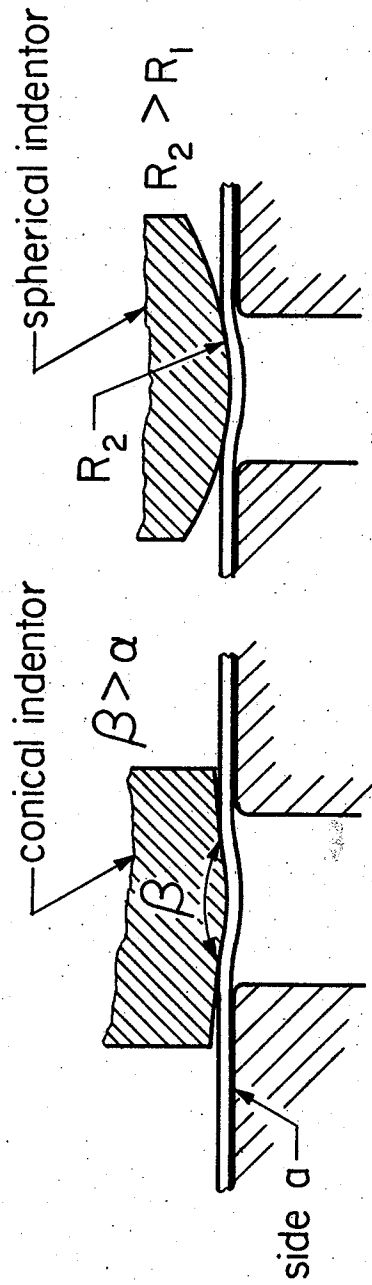


Figure 3.1 Concentric Dimpling



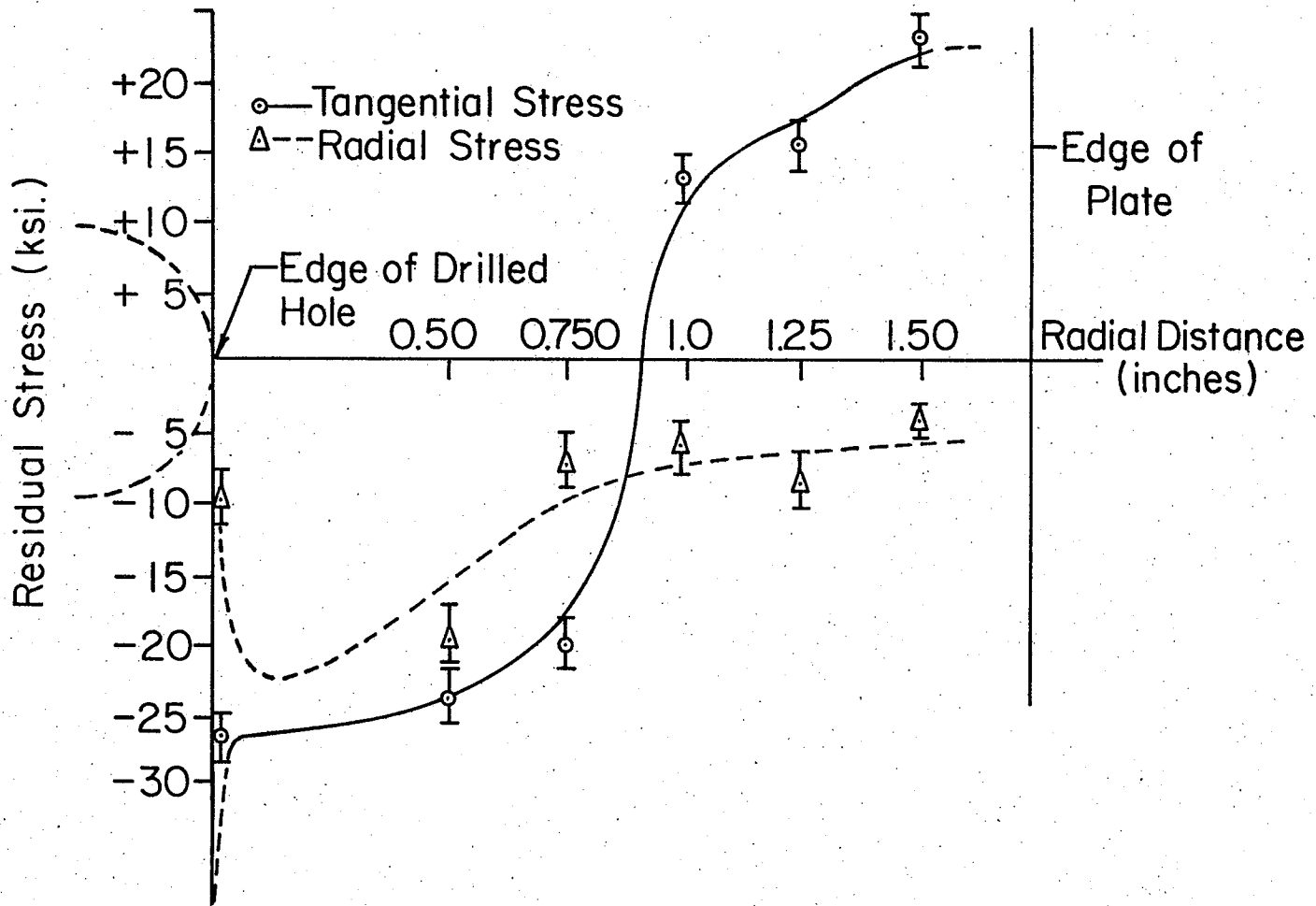
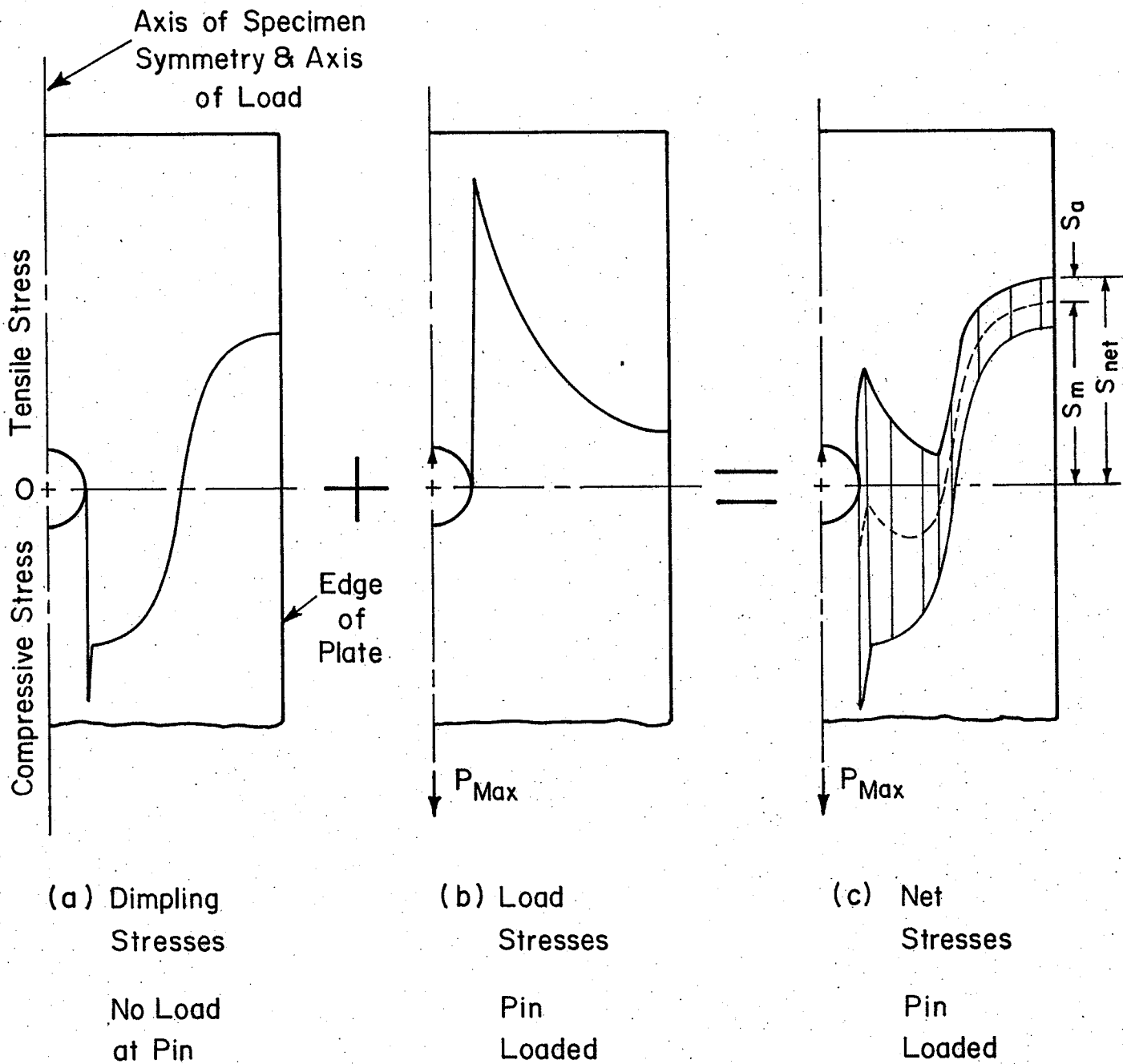


Figure 3.2 Optimum Dimpling Residual Stresses (14)

thought that the residual compressive stresses may approach the yield point of the material. Figure 3.3 demonstrates schematically the superposition of the tensile hoop stresses of a maximum load onto the residual hoop stresses produced by dimpling. The net stresses in (c) result. Notice that in the critical region near the hole boundary, the high residual compressive stresses have significantly reduced the load stresses while in the lower stressed region away from the hole boundary the low load stresses have not increased the high residual tensile stresses to any great extent. The end effect is a lowering of the mean stresses in the critically stressed region accompanied by an improvement in the fatigue strength of the component.

### 3.3 The Interference Mechanism

An interference fit, produced by insertion of an oversized pin into a given size hole of a plate, increases the mean hoop stresses, but significantly lowers the alternating stresses in the plate so that a preferable stress state is produced. Interference fits also reduce the amount of relative movement or slip between points of contact at the hole boundary and thus act as a deterrent to fretting fatigue. The reduction of the alternating stresses in the critically stressed regions of a simple pin joint or lug was explained by Heywood (16) with the aid of Figure 3.4. With no load at the pin, an interference-fit pin produces tensile hoop stresses (represented by the curve) and a radial compressive stress field in the lug material about the hole. When an external pin load is applied,




 Reveals ranges of hoop stress over the specimen cross section.

Figure 3.3 Dimpling Mechanism

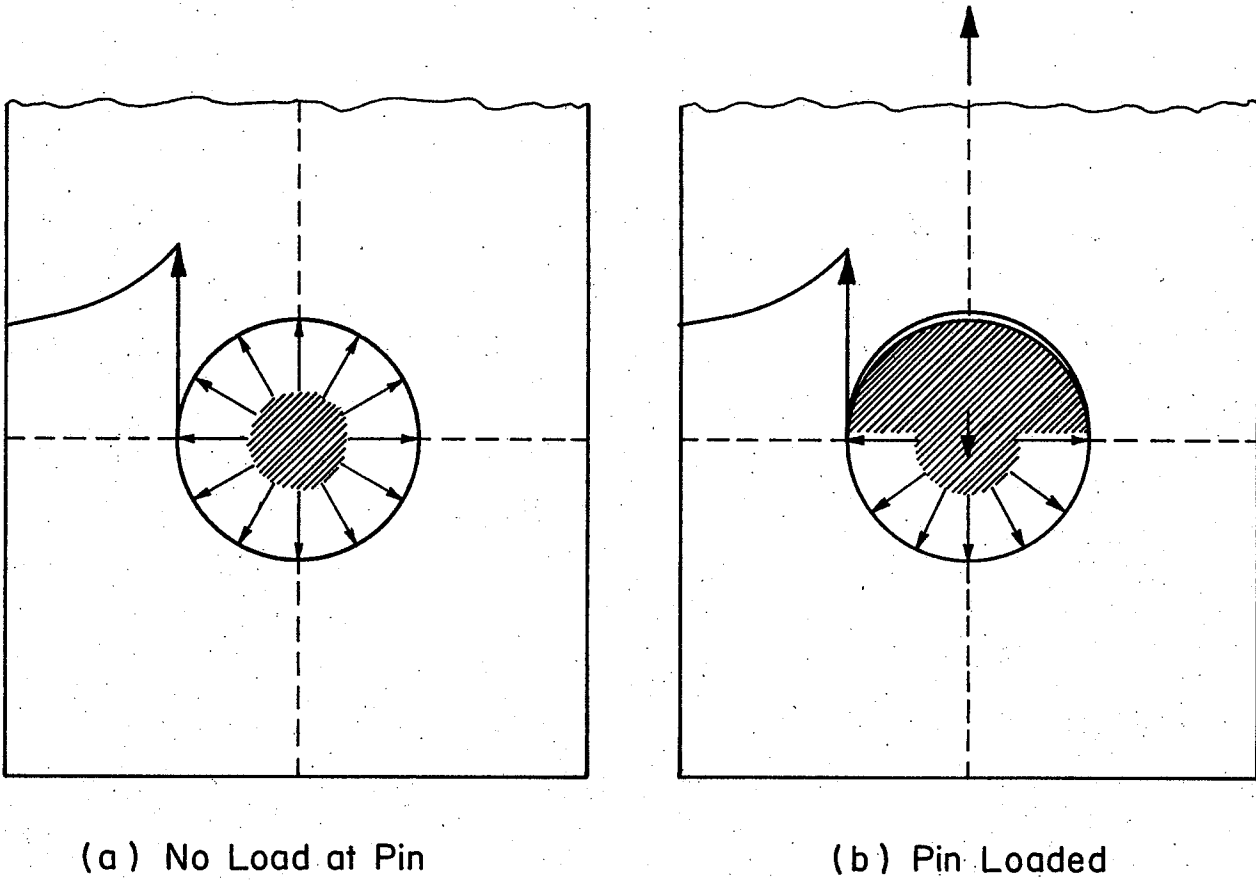


Figure 3.4 Interference Mechanism

the radial compressive stresses on the unloaded side of the hole are reduced as shown at (b), with only a little increase in the stresses on the side in the direction of loading. In effect, the radial compressive stresses on the unloaded side of the hole (forcing the pin in the direction of loading) have been replaced with an equivalent pin load while therefore insignificantly altering the stresses in the critical minimum section. The schematic hoop stress versus pin load curve of Figure 2.4 usually results. Stresses within the elastic limit are considered.

### 3.4 The Dimpling-Interference Mechanism

By combining an interference fit with dimpling, either both the stress range and maximum hoop stress or both the alternating and mean hoop stresses within the plate material in the critical region about the hole should be reduced, subsequently yielding a greater fatigue life than either method alone could produce. Employing the Goodman-type fatigue-strength diagram of Figure 3.5 constructed from unnotched data for 2024-T3 alclad aluminum alloy sheet given in (15), the four specimens in Figure 3.6 are compared using superposition of stresses. Failure is assumed to begin at the hole boundary of the minimum net section. It is recognized that the fatigue strength reduction factor does not remain constant over the entire range of fatigue life. However, as a matter of convenience, the same load stresses will be applied to each specimen for the purpose of postulating a mechanism. It is also assumed here that the plate material will not experience any fluctuation in hoop stress at any point in the

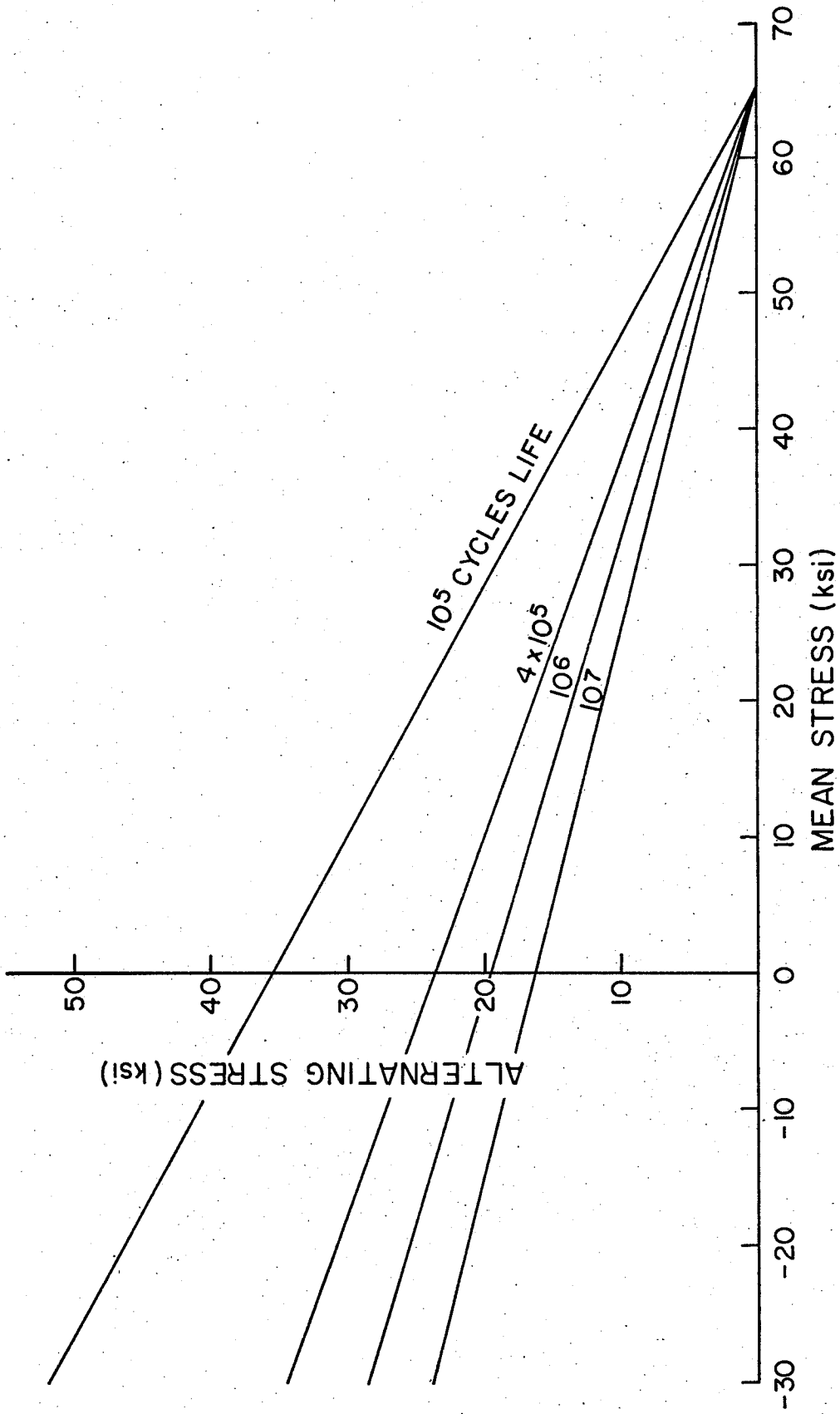


Figure 3.5 Goodman-Type Fatigue-Strength Diagram Constructed from Unnotched Data for 2024-T3 Alclad Aluminum Alloy Sheet (15)

- (1) Load Stresses
- (2) Interference Stresses
- (3) Resultant Stresses
- (4) Dimpling Stresses
- (5) Dimpling + Interference Stresses

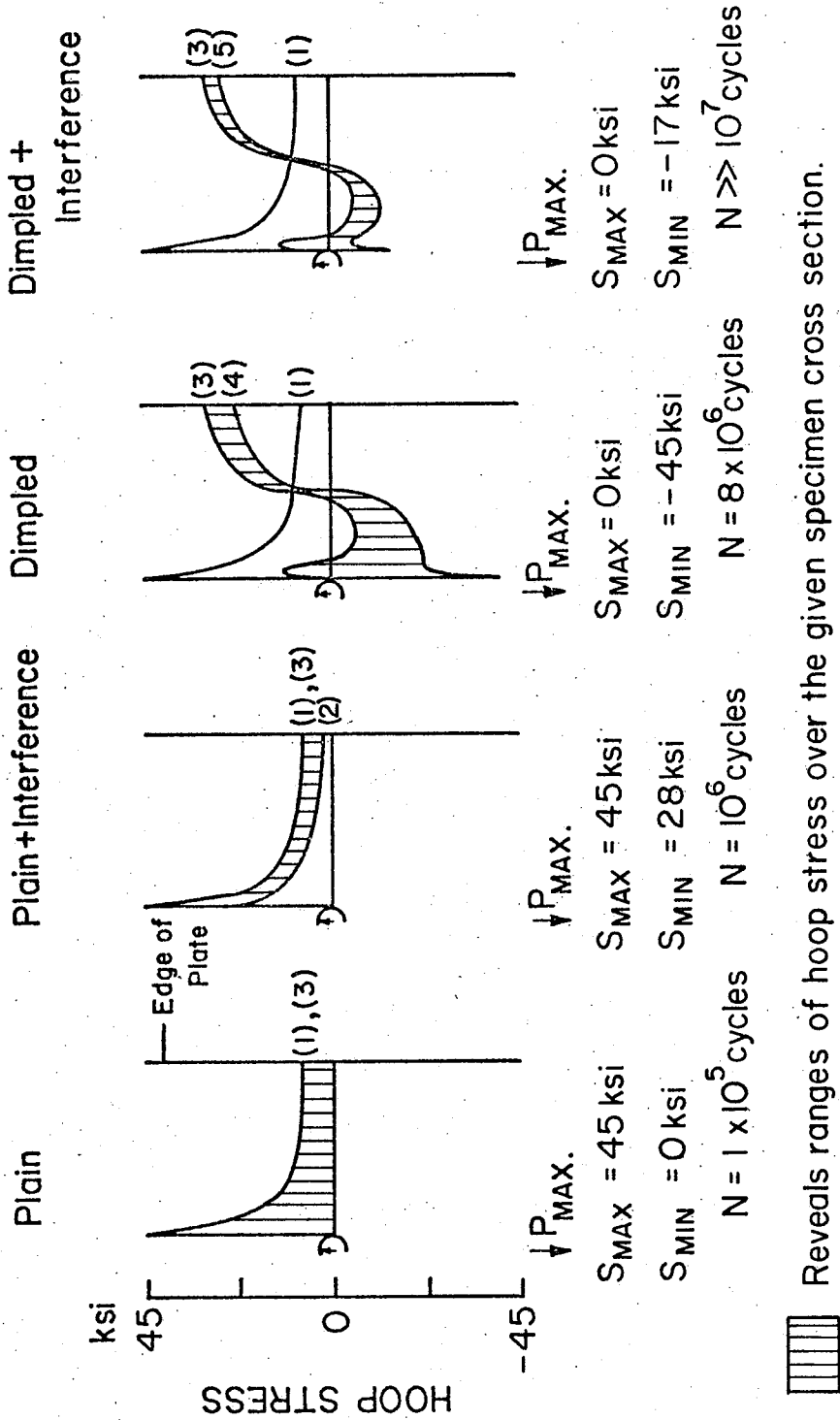


Figure 3.6 Dimpling-Interference Mechanism

minimum section until the load hoop stress exceeds the initial interference hoop stress at that point due to the interference mechanism. Minimum and maximum hoop stresses experienced at the hole boundary of the minimum net section are listed for each specimen. According to Figure 3.5, the dimpled specimen with interference would endure the highest number of load applications. Looking at the last assumption, it also becomes obvious that the interference which is able to create hoop stresses most nearly approximating the applied load maximum hoop stresses especially in the critical region about the hole would represent the optimum interference since the least severe static-load condition would then be approached, thereby reducing or eliminating the possibility of a failure initiating at the point in question.

### 3.5 Closure

Considering the beneficial effects of interference and dimpling on the fatigue strength of pin-loaded holes, and the relative independence of the two mechanisms, it was postulated that further fatigue strengthening is possible by combining dimpling with interference.



## CHAPTER 4

## EXPERIMENTAL STUDY

4.1 Introduction

An experimental program was carried out to evaluate the combined effect of an interference fit and dimpling on the loaded hole fatigue strength of thin aluminum sheet. Specimen material, type of loading, and close dimensional similitude were maintained in one-to-one correspondence with the work done by Shewchuk and Roberts (14).

4.2 Test Program

The investigation was designed to present the following information for a pin-loaded specimen of given material and configuration but in varying preparation or condition:

- (1) An S-N curve for plain specimens utilizing exact-fit pins
- (2) An S-N curve for dimpled specimens utilizing exact fit pins
- (3) The optimum interference, based on fatigue tests, for dimpled specimens at each stress level equal to and/or above those in (2)
- (4) An S-N curve for dimpled specimens utilizing the optimum interference fits dictated by (3).

From these curves, the performance expressed in terms of fatigue strength of each specimen condition relative to the others could be ascertained.

### 4.3 Test Details

#### 4.3.1 Material and Specimens

The specimens were prepared from commercially available 2024-T3 alclad aluminum alloy sheet. Table 4.1 lists the nominal chemical composition and mechanical properties of the material. The mechanical properties, as determined from laboratory tensile tests, are also entered in Table 4.1. Interference and exact fits were provided by ground, 4140 alloy-steel tapered pins with a Rockwell C hardness between 42 and 46. The taper was 0.0208 inch per inch.

The specimen dimensions and orientation with regard to the rolling direction are shown in Figure 4.1.

#### 4.3.2 Specimen Preparation

Blank specimens were first rough cut to the appropriate length from the sheet using a shear press. These were subsequently milled from one edge to the required transverse dimension.

The dimpling procedure, in the order in which it was performed, is shown in Figures 4.2 to 4.4. The combination of dimpling parameters in Figure 4.2 correspond to the optimum found by Shewchuk and Roberts (14). The operations in Figures 4.3 and 4.4 were employed to successfully flatten the dimple. Clearances of 0.017 and 0.014 inch existed between the specimen and the loading fork prior to and after dimpling respectively.

TABLE 4.1

Nominal Chemical and Mechanical Properties  
of 2024-T3 Alclad Aluminum Alloy Sheet (17).

Nominal Chemical Properties

Cu	4.5%
Mg	1.5%
Mn	0.6%

Nominal Mechanical Properties

Ultimate Tensile Strength	65,000 psi.
Yield Strength	45,000 psi.
Hardness	E 90-100
Fatigue Limit (unclad)	20,000 psi.
@ 500 x 10 <sup>6</sup> cycles	
R. R. Moore Rotating Bending	
Modulus of Elasticity	10.6 x 10 <sup>6</sup> psi.

Mechanical Properties as Determined  
From Laboratory Tensile Tests

Ultimate Tensile Strength	64,300/65,600 psi.
Yield Strength (0.2% offset strain)	42,100/42,500 psi.
Elongation in 1 inch, %	19/19
Modulus of Elasticity	10.5 x 10 <sup>6</sup> /10.7 x 10 <sup>6</sup> psi.

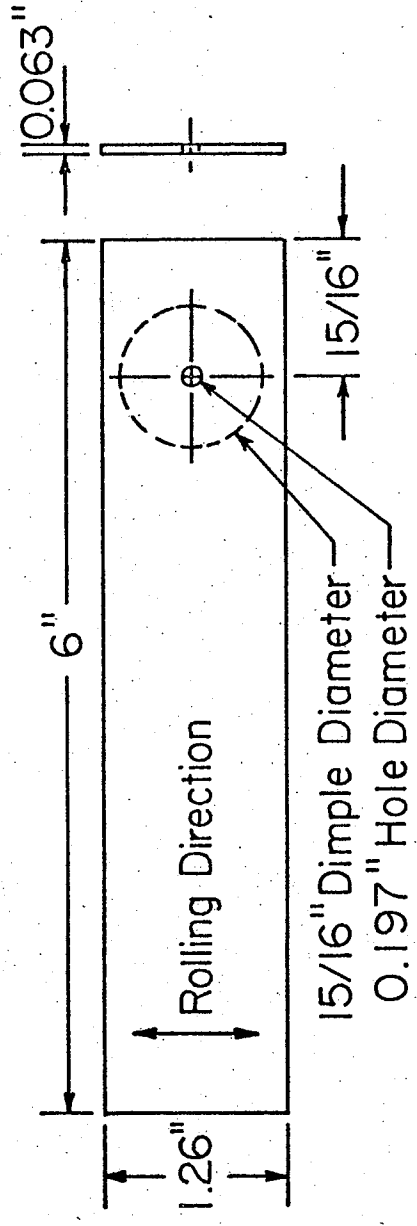


Figure 4.1 Test Specimen

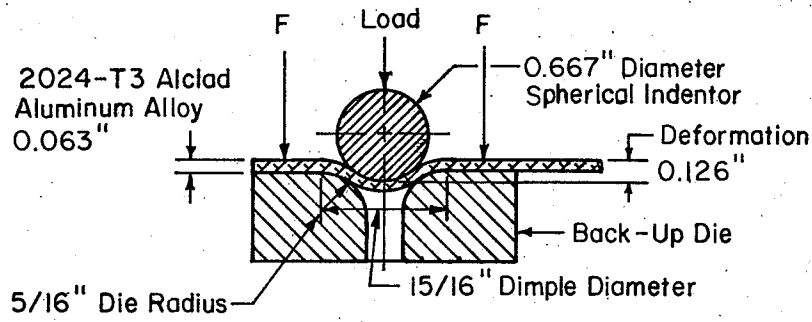


Figure 4.2 Dimpling - Indentation.

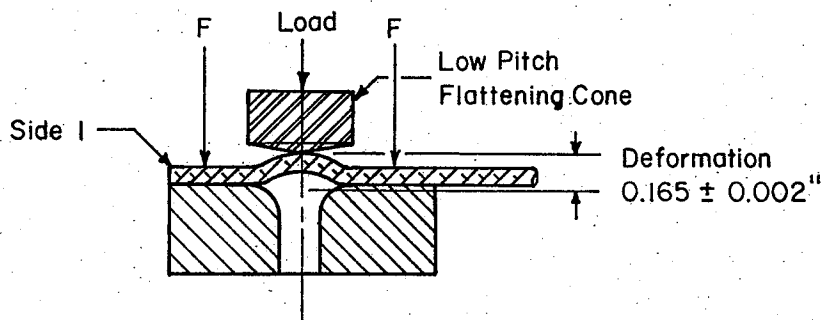


Figure 4.3 Dimpling - First stage flattening

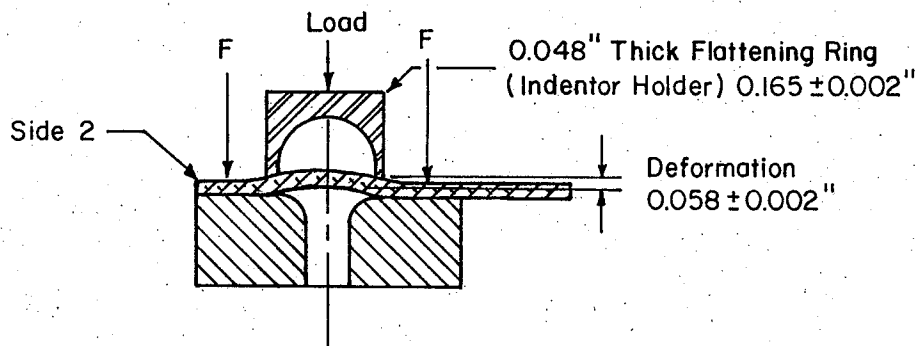


Figure 4.4 Dimpling - Second stage flattening.

Hole preparation was performed in two stages. First, an under-sized hole was drilled using a center drill, centered initially by a specimen hole accurately located with the same center drill on a milling machine. The existing hole was then reamed to the proper size with a tapered reamer, the proper size being supplied by the appropriate advancement of the reamer from contact with the top surface of the specimen to the vertical depth indicated by a dial on the drill press, accurate to  $\pm 1/32$  inch, and determined on the basis of the reamer dimensions specified by the manufacturer. The taper was again 0.0208 inch per inch. The general set-up is displayed in Figure 4.5. Further, any burr remaining on the hole after reaming was gently removed with 600A grit paper.

#### 4.3.3 Interference Technique

The degree of interference was governed by the appropriate amount of forced relative displacement of the tapered pin through the specimen hole as suggested in Figure 4.6. The tapered holes in the loading fork were reamed to afford a loose fit between the pin and the loading fork up to a maximum interference of 9 percent in the specimen.

#### 4.3.4 Test Procedure

In keeping with the test program, three types of specimen condition were tested - plain, dimpled, and dimpled with interference. Interference levels for the dimpled specimens were appropriately varied to establish the optimum interference for the majority of the given nominal applied

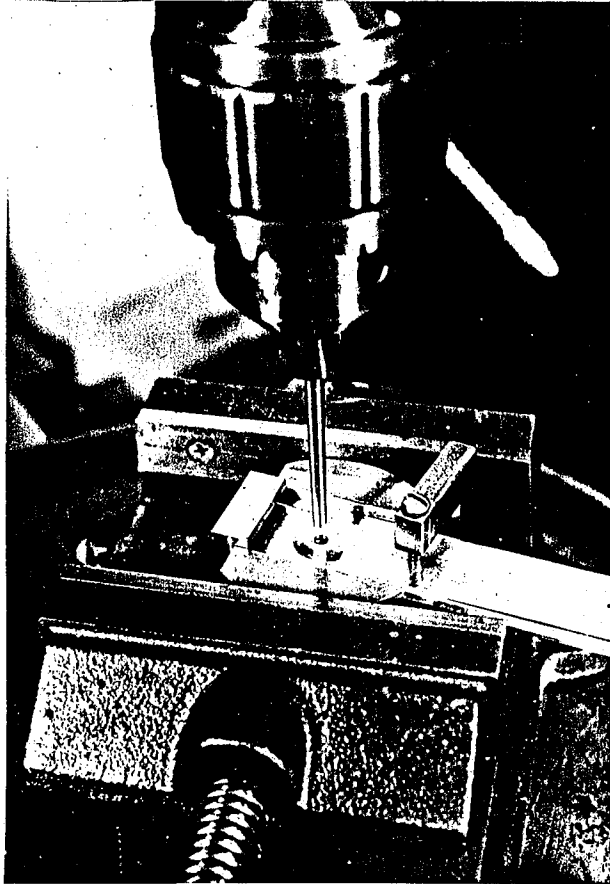


Figure 4.5 Hole Preparation - Reaming

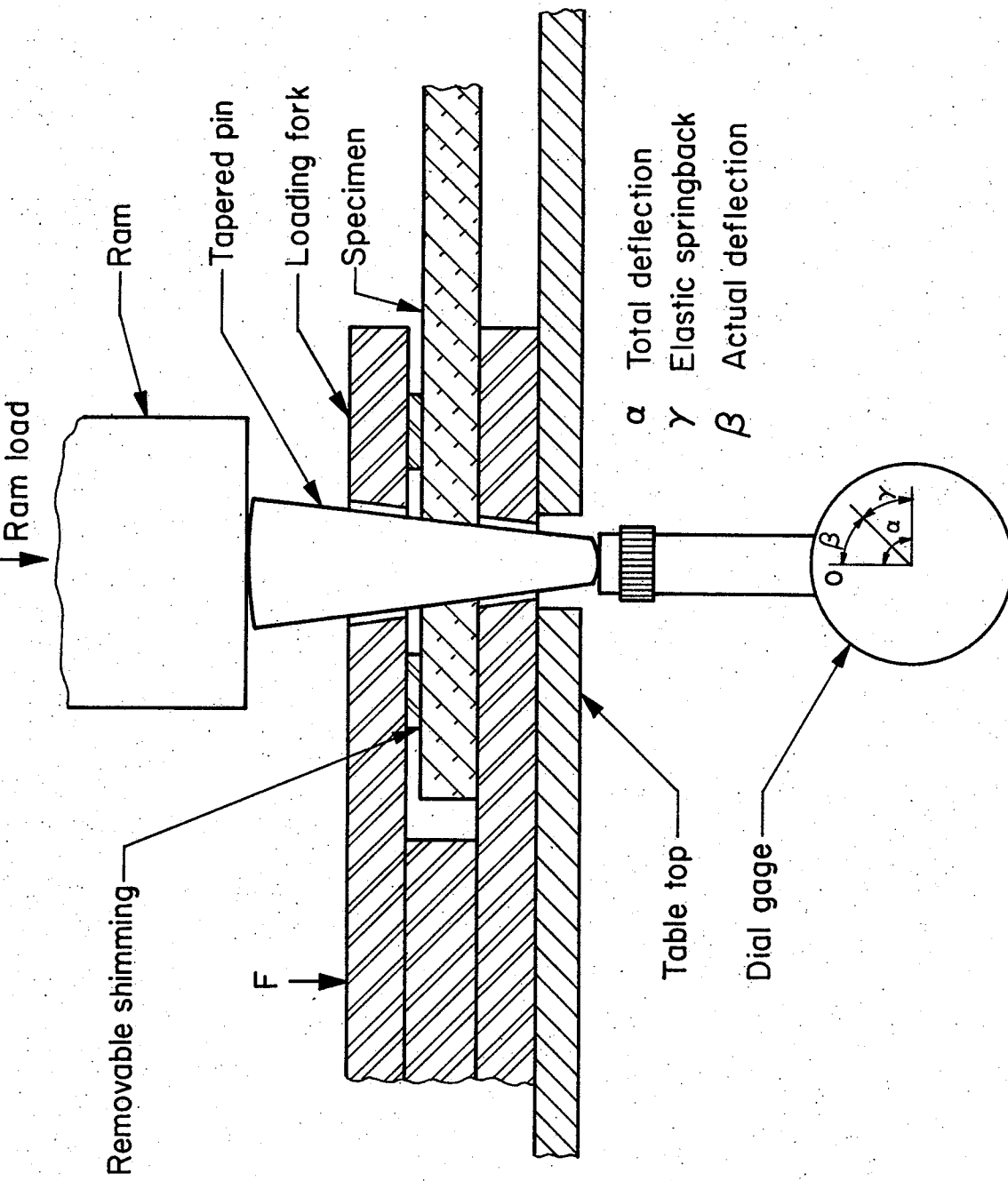


Figure 4.6 Interference Technique



stress levels. In addition, several preliminary tests were performed on plain specimens with interference in order to substantiate the interference technique. The specimens were all cycled in zero-to-tension fatigue tests at 100 Hz in an Amsler Vibrophore. Each specimen was cycled continuously until fracture. Figure 4.7 shows the loading arrangement.

#### 4.4 Test Results

The results of the interference optimization testing and the associated S-N curves are presented in Figures 4.8 and 4.9 respectively. Table 4.2 lists the results of the fatigue tests performed on plain specimens with and without pin interference.

Unnotched data for 2024-T3 clad aluminum alloy sheet (15) and the dimpled specimen curve from Shewchuk and Roberts (14) are also included in Figure 4.9 for later analysis and comparison purposes.

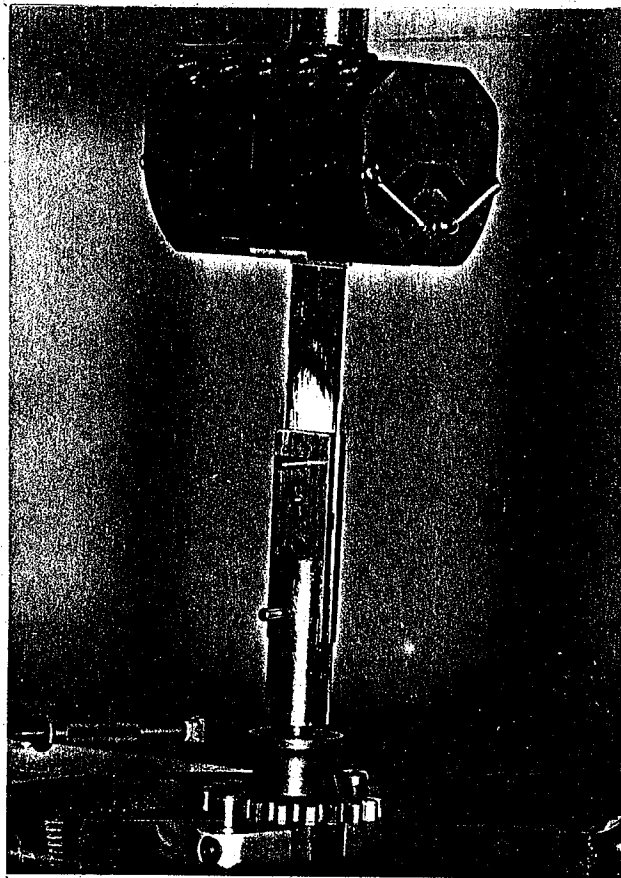
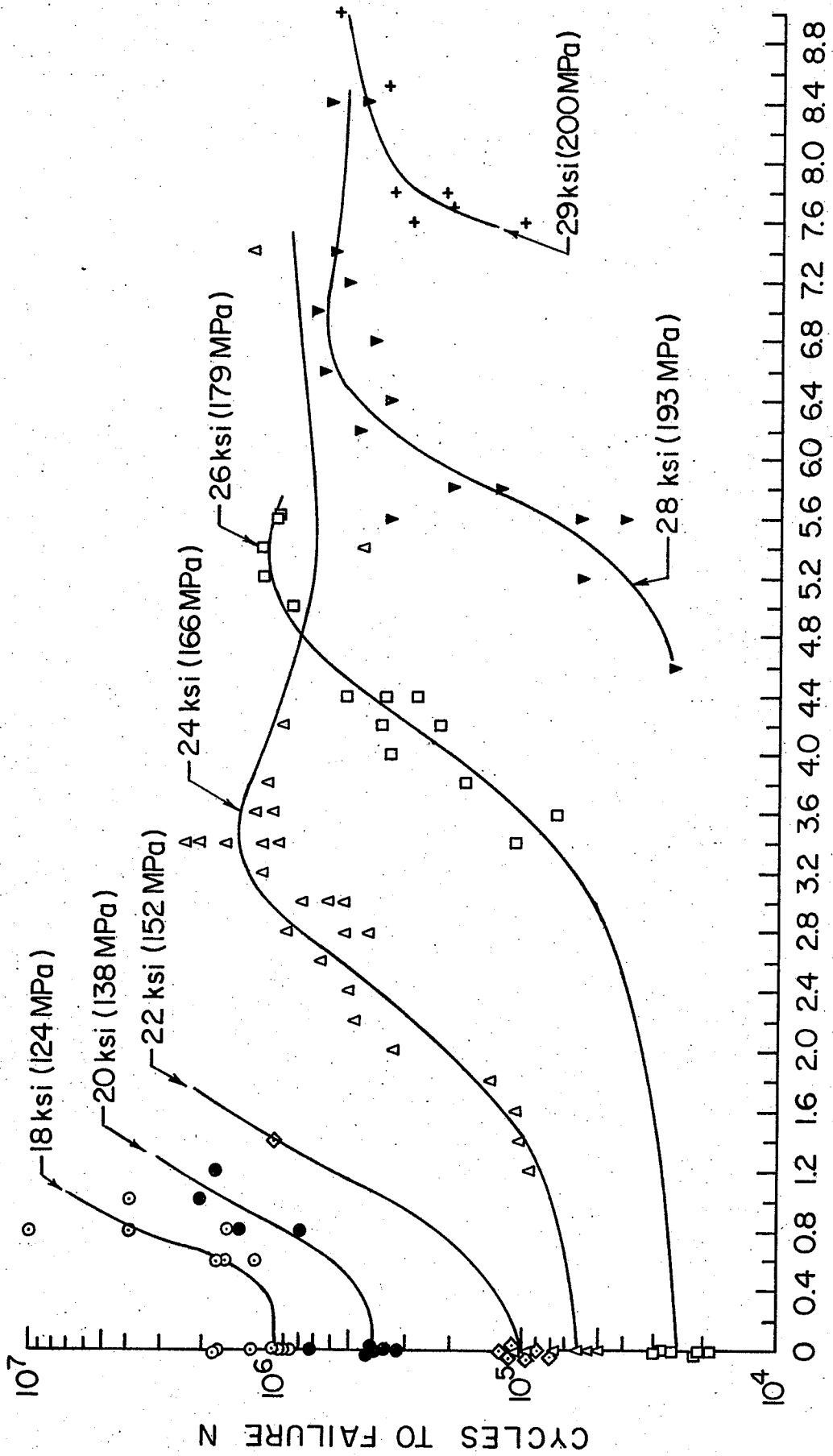


Figure 4.7 Loading Arrangement



INTERFERENCE (% HOLE DIAMETER)

Figure 4.8 Dimpled Specimen Interference Optimization Results

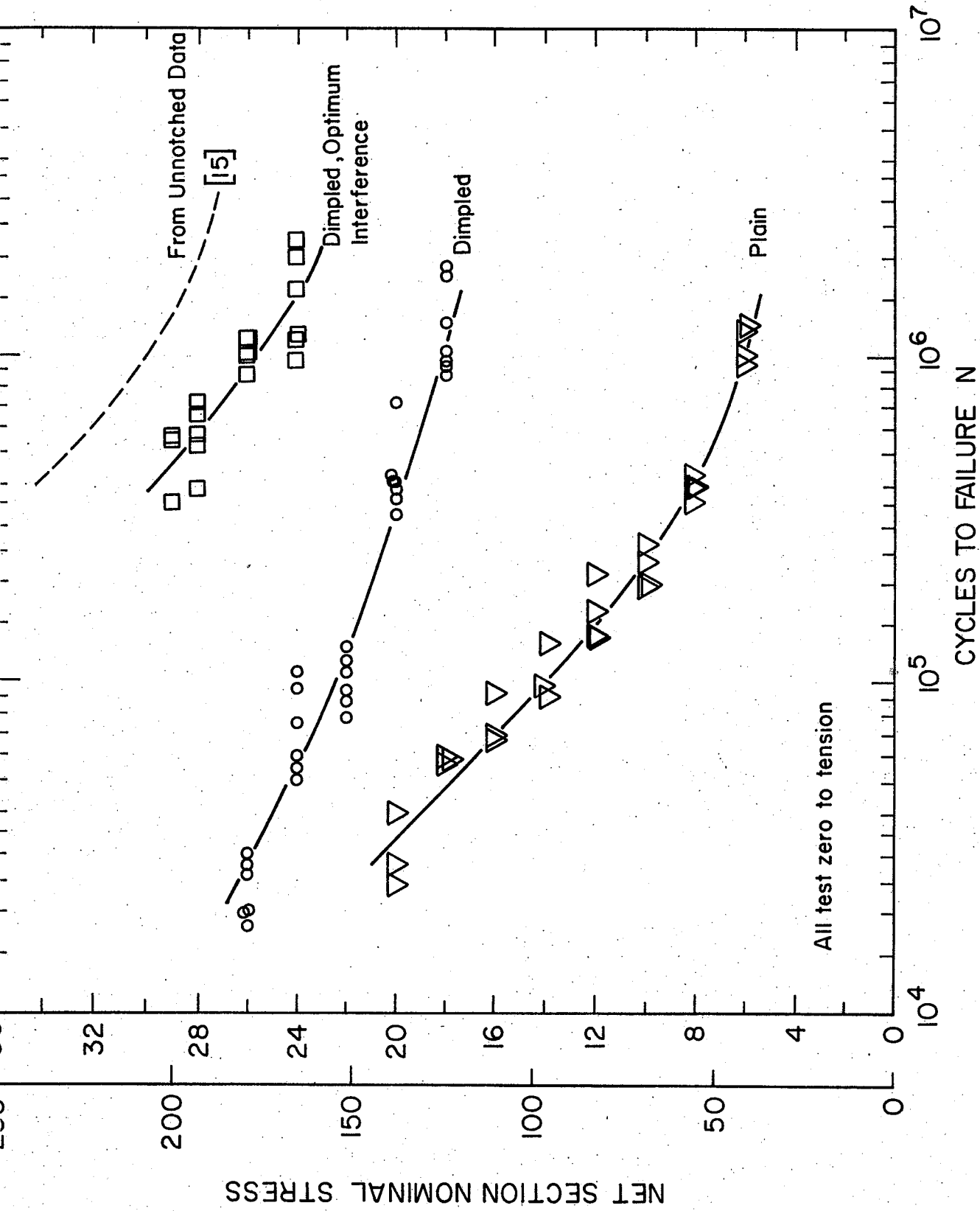


Figure 4.9 Fatigue Test Results

TABLE 4.2

Results of Fatigue Tests on Plain Specimens  
With and Without Pin Interference

Stress (ksi)	Interference (inch/inch)	Cycles to Failure, N
6	0.000	1,265,000/1,307,000/1,000,000/920,000
8	0.000	355,000/400,000/395,000/425,000
	0.006	751,000/1,820,000/450,000/1,463,000
10	0.000	189,000/200,000/262,000/230,000
12	0.000	140,000/138,000/215,000/167,000
	0.004	218,000/190,000
	0.005	249,000/220,000/200,000
14	0.000	90,000/98,000/135,000
	0.004	121,500
	0.005	132,000/133,000
	0.006	123,000
16	0.000	67,000/68,000/92,000
	0.004	86,000
	0.005	106,000
	0.006	116,000/97,500/107,500/113,000
	0.007	84,500
	0.008	102,500/106,500/97,500
	0.010	210,000/83,500
	0.014	420,000
	0.018	885,000
	0.024	1,715,000
18	0.000	61,000/55,000/58,000
	0.004	67,000
	0.006	88,500
	0.048	3,900,000 (No Failure)
20	0.000	24,000/28,000/40,000

## CHAPTER 5

## ANALYSIS OF RESULTS

5.1 Introduction

A discussion of the test results presented in the previous chapter will now be conducted under the following headings:

- (1) Dimpling
- (2) Interference Technique
- (3) Interference Optimization
- (4) Dimpling with Optimum Interference
- (5) Interference versus Crack Location
- (6) Prediction of Fatigue Strength and Life.

5.2 Dimpling

According to Figure 4.9, dimpling creates a strength improvement factor of 2.85 at  $10^6$  cycles to failure. The strengthening effect is due to the ability of the compressive stresses, set up by the dimpling process about the loaded hole, to counteract any applied tensile stresses therein and thereby reduce the magnitudes of the net and mean stresses. The strengthening effect of dimpling, however, becomes progressively lower as the fatigue life decreases.

In the present dimpling process, a different flattening procedure was employed in lieu of the one used by Shewchuk and Roberts (14). Following the latter method gave rise to longitudinal bowing in the specimen

test section containing the treated material. A comparison of the present dimpled specimen curve to that of the above investigators, however, shows the two curves to be in close agreement.

### 5.3 Interference Technique

To obtain a high range in levels of interference, tapered pins were used in the present experimental investigation in preference to chamfered pins of the type used by (9) and (10). It is postulated that damage induced in the plate material surrounding the hole by the gradual forced entry of a fully tapered pin is smaller as compared to that created by pressing through a plain drilled hole, a proper size pin having an initial entry chamfer. Pinhole damage produced by the latter was reported by Smith (10) for an interference level as low as 0.006 inch per inch when an insufficient entry length at a  $10^\circ$  chamfer was used. In the present case, extrusion of plate material from the hole in the form of a slight ridge was not noticeable until an interference of approximately 4 percent of hole diameter. In addition, with tapered pins, the recurring need to match the proper size pin to a hole of known measured diameter to give the desired interference was eliminated. Further, for the taper and plate thickness used, the difference between the degrees of interference at both ends of the specimen hole was negligible.

Some insight into the performance of the technique may be obtained from a comparison of the present results of tests performed on plain specimens with interference to those of Hartman and Jacobs (8), Low (9), and Smith (10). Before a comparison can be made, however, differences in material; lug geometry, and interference levels must somehow be accounted for. In an attempt to accomplish this, the following approach is adopted here in which two dimensionless stress ratios are employed. These are:

$$\frac{S_{MAX}}{S_{INT}} = \frac{K_f \times S_{NOM}}{S_{INT}}$$

and

$$\frac{S_{INT}}{S_Y}$$

where  $S_{MAX}$  = maximum load hoop stress at the hole boundary of the minimum net section

$K_f$  = fatigue strength reduction factor

$S_{NOM}$  = nominal applied stress over the minimum net section

$S_{INT}$  = initial interference hoop stress at the hole boundary of the minimum net section

$S_Y$  = yield stress of the given material.

The first ratio gives an indication of the degree of loading for the given interference. The second gives an indication of the degree of interference.



Maximum load and initial interference hoop stresses are computed as elastic stresses regardless of whether or not the actual yield point of the material is exceeded. Good agreement between investigations is considered to exist when, for identical corresponding stress ratios, the specimens of each fail at the same life. What is involved, therefore, is to establish the equivalent levels of interference and corresponding applied stresses at a given life for the present investigation from the stress ratios of the others at the same life. A comparison is then made with the available present experimental results at the life in question.

Fatigue strength reduction factors,  $K_f$ , are calculated from Neuber's equation for holes

$$K_f = 1 + \frac{K_t - 1}{1 + (a/r)^{1/2}} \quad (5.1)$$

where

$K_t$  = theoretical stress concentration factor

$a$  = empirical constant representing the half length of a fictitious "building block" or "equivalent grain" of the material, inches

and

$r$  = radius of the hole, inches.

Theoretical stress concentration factors for the various dimensional combinations of the specimens are established from the curves in Figure 5.1 extracted from Heywood (16). Values for the empirical constant are obtained from the curves in Figure 5.2 reported in Juvinal (18). The

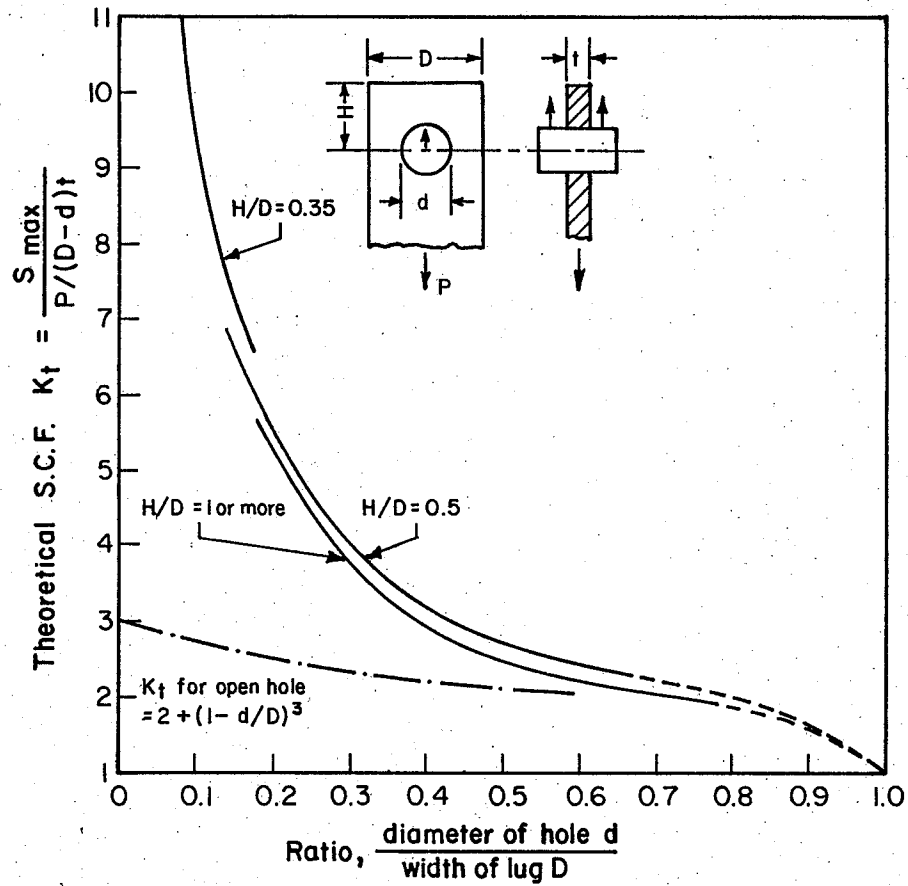


Figure 5.1 Theoretical Stress Concentration Factors,  $K_t$ , for Loaded Lugs With Small Clearance Between Hole and Pin

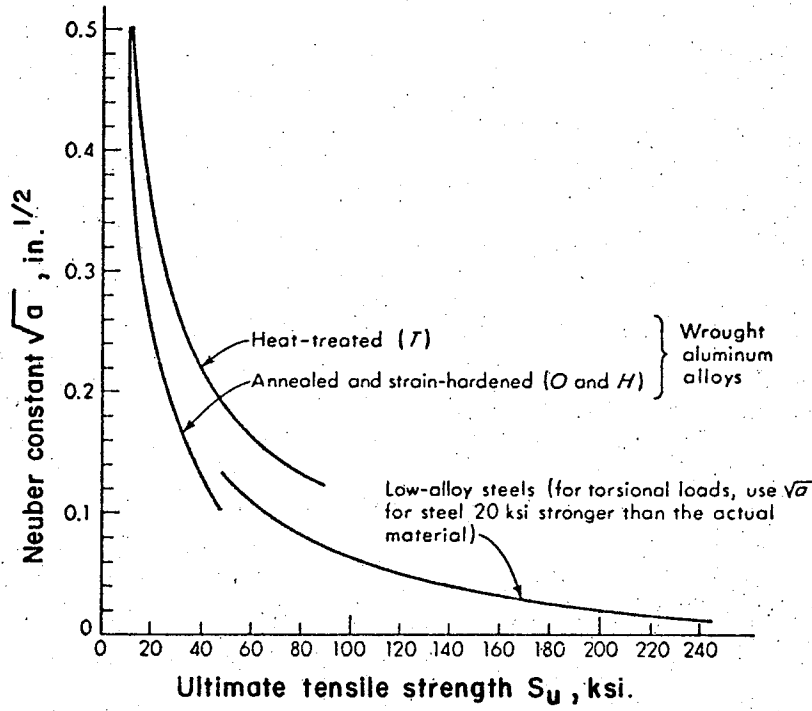


Figure 5.2 Neuber Constants for Steel and Aluminum

calculated fatigue strength reduction factors for the present and aforesaid investigations are given in Table 5.1 along with the specimen dimensions and theoretical stress concentration factors.

Initial interference hoop stresses at the hole boundary are tabulated from the Lamé thick cylinder theory as applied to shrink fits. Lambert (19), employing photoelasticity, has shown that for ratios of hole diameter to plate width ( $d/D$ ) of less than 0.6, the Lamé theory sensibly predicts the principal stresses on the hole boundary due to an interference-fit pin in a rectangular plate of finite width. The initial interference hoop stresses at the hole boundary for the four investigations are given in Table 5.2 for the levels of interference tested.

The results of the analysis for  $10^6$  cycles to failure are entered in Table 5.3. Present experimental fatigue strengths agree to within 18.5 percent of the required values for equivalent or nearly equivalent levels of interference. Of some note also is the close agreement between Low, and Hartman and Jacobs via the present experimental investigation.

#### 5.4 Interference Optimization

Referring to Figure 4.8, each stress level appears to have an optimum interference. That is, an interference fit at which the loaded hole can sustain the highest number of load applications for the given loading. Below the optimum, the fatigue life of the component increases with increasing interference. Above the optimum, the component suffers an initial decline in fatigue life from the maximum before the latter apparently stabilizes at a level which still represents a substantial improvement.

TABLE 5.1

Calculated  $K_f$  Values for Loaded-Hole Specimens

Investigation	Specimen Dimensions			$K_t$	$K_f$
	d(in.)	D(in.)	H(in.)		
Present Investigation	0.1976	1.26	0.945	6.35	4.53
Low (9)	1.000	2.25	1.500	2.70	2.49
Hartman & Jacobs (8)	0.236	1.18	0.787	5.50	4.07
	0.394	1.18	0.787	3.50	2.84
Smith (10)	1.250	3.75	1.875	3.50	3.15

TABLE 5.2

## Interference Hole Boundary Hoop Stresses for Loaded-Hole Specimens

Investigation	Material	$S_y$	Interference, inch/inch	Hole Boundary Hoop Stress (ksi.)
Present Investigation	2024-T3	43	0.005	34.6
			0.006	41.5
			0.010	69.2
			0.014	96.9
			0.018	124.6
			0.024	166.1
Low (9)	B.S. L65	58	0.002	29.6
			0.004	59.1
			0.007	103.4
			0.010	147.8
Hartman & Jacobs (8)	24S-T	50	0.0025	17.5
			0.0067	46.8
Smith (10)	24S-T	50	0.0040	29.0
	7075-T6	75	0.006 (1/8 in. bushing)	25.3
			0.006 (1/4 in. bushing)	35.2

TABLE 5.3

Comparison of Present Investigation to Low (9), Hartman & Jacobs (8),  
and Smith (10) at  $10^6$  Cycles to Failure

Investigation	Interference (inch/inch)	$\frac{S_{MAX}}{S_{INT}}$	$\frac{S_{INT}}{S_y}$	Required Conditions for Present Investigation		Present Experimental Results		
				Int. (in./in.)	$S_{NOM}$ (ksi.)	Int. (in./in.)	$S_{NOM}$ (ksi.)	Median Life (cycles)
Low (9)	0.002	1.330	0.510	0.0032	6.4	0.000	6.3	$1.0 \times 10^6$
	0.004	1.015	1.019	0.0063	9.8	0.006	8.0	$1.1 \times 10^6$
	0.007	0.722	1.783	0.0111	12.2	0.006	8.0	$1.1 \times 10^6$
	0.010	0.547	2.548	0.0158	13.2	0.005	12.0	$2.2 \times 10^5$
Hartman & Jacobs (8)	0.004	1.498	0.580	0.0036	8.2	0.000	6.3	$1.0 \times 10^6$
Hartman & Jacobs (8)	0.0025	1.861	0.350	0.0022	6.2	0.000	6.3	$1.0 \times 10^6$
	0.0067	1.104	0.936	0.0058	9.8	0.006	8.0	$1.1 \times 10^6$
Smith (10)	0.006 (1/8 in. bushing)	2.341	0.337	0.0021	7.5	0.000	6.3	$1.0 \times 10^6$
	0.006 (1/4 in. bushing)	1.682	0.469	0.0029	7.5	0.000	6.3	$1.0 \times 10^6$

Interference levels considerably higher than previously investigated were used to provide the improvements in strength. These were required to prevent hole elongation in the specimens under the initial load applications that would reduce to some extent or entirely the amount of plate material under radial compression at zero load on the unloaded side of the hole. To prevent hole elongations at higher load levels, more interference is required. Failure to do so, would result in less than optimum strengthening with decrease in life. This is also demonstrated by the constant life curves of Low (9) in Figure 2.7.

#### 5.5 Dimpling with Optimum Interference

From Figure 4.9, optimum tapered-pin interference increases the dimpled, loaded-hole fatigue strength by approximately 40 percent at  $10^6$  cycles to failure and relative to the plain specimen at this life, it represents a fatigue strength improvement factor of 4.0. With the addition of the 'unloading effect' of an interference fit, fluctuations in stresses experienced by the plate material are reduced. In addition, shear stresses set up at the hole boundary by an interference fit reduce the amount of relative motion between the pin and the plate and thus act as a deterrent to fretting as well as possibly prevent to some extent the opening up, under load, of hole boundary microcracks. The strengthening effect with respect to the plain specimen, again, decreases with decrease in life.



The fatigue strength reduction factors at  $10^6$  cycles to failure are found to be:

Plain	4.76
Dimpled	1.67
Dimpled, Optimum Interference	1.18

Thus it is seen that the combined technique provides a most significant fatigue strength improvement.

### 5.6 Interference versus Crack Location

The effect of interference on crack location in failed, dimpled specimens for three stress levels is illustrated in Figure 5.3. Zero-interference specimens appear to fail either on or slightly ahead of the horizontal centre-line where fretting occurs and maximum stress range and possibly maximum stress are highest. Both fretting and cracking continually shift toward the unloaded side of the hole with increasing interference until the interference essentially nullifies the stress-concentrating effect of the hole by reducing the alternating stresses as well as the degree of fretting, but leads to failure of the specimen within or across the dimple diameter behind the hole where the combination of mean and alternating stresses must produce a more unfavorable stress state.

### 5.7 Prediction of Fatigue Strength and Life

The fatigue strength of dimpled loaded holes will now be estimated for the cases of a push-fit and an interference-fit pin. The method employed by Shewchuk and Roberts (14) is selected in favor of other

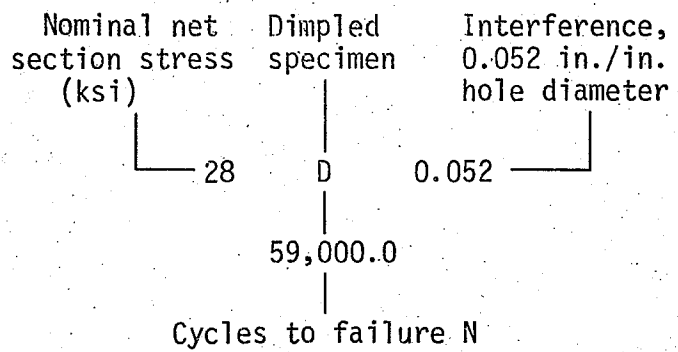
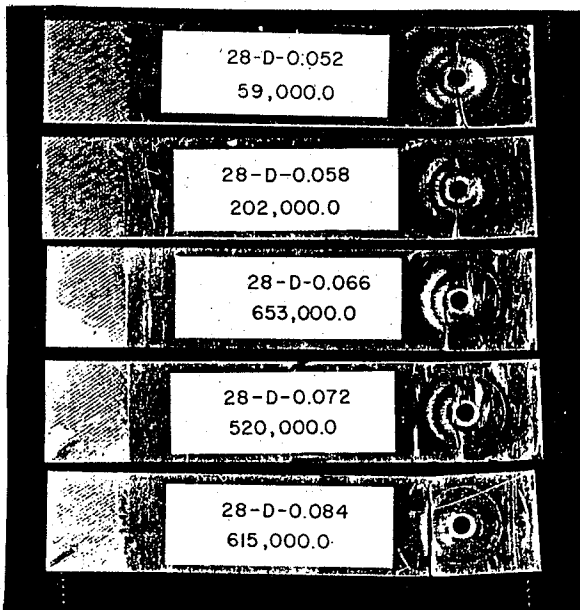
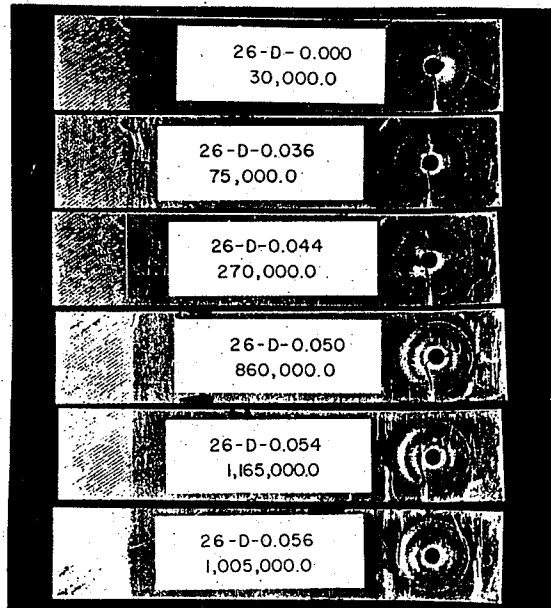
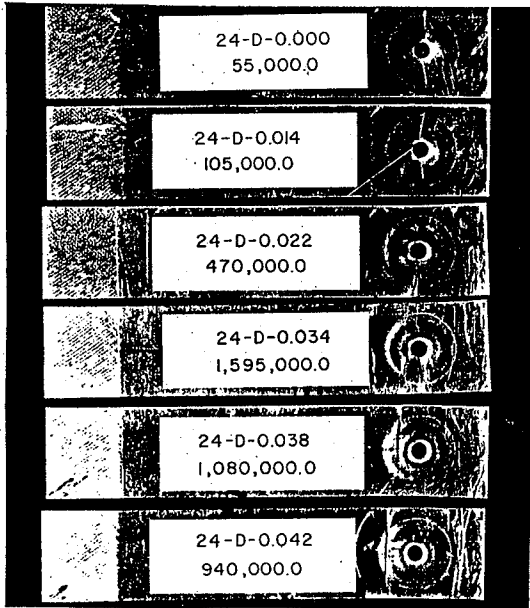


Figure 5.3 Interference Versus Crack Location

approaches since it has been shown to reasonably predict the dimpled loaded-hole fatigue strength for the former case. Additions are included in the method when considering an interference fit. In each case, failure is assumed to occur at the minimum net section. Predicted values and experimental results are compared.

(a) Dimpled; Push-Fit Pin

The method employed by (14) is demonstrated graphically in Figure 5.4. One begins by constructing a Goodman line for the desired life, line AB, on  $S_a$ - $S_m$  coordinates. In order to work with nominal applied stresses in the presence of a stress concentration, a new line DE is drawn parallel to line AB but shifted according to the associated fatigue strength reduction factor as shown in the Figure. A residual stress immediately adjacent to the stress concentration is then treated as an externally applied nominal stress causing a shift DF in the origin on the mean stress axis equal to the amount of the residual stress. This approach might seem warranted for dimpling due to the broad residual stress profile produced in the plate material near the hole boundary. In other words, failure does not necessarily need to be based on the stresses at the hole boundary for the case of a broad residual stress profile about the hole. A line of slope corresponding to the ratio of  $S_a/S_m$  is drawn next intersecting ED at G. The point G or H on the  $S_a$  axis defines the permissible nominal alternating stress for the loading ratio or condition  $P_a/P_m$  for the life in question. Note that for a loaded hole with a push-fit pin, the applied stress ratio  $S_a/S_m$  is identical to the load ratio  $P_a/P_m$ .

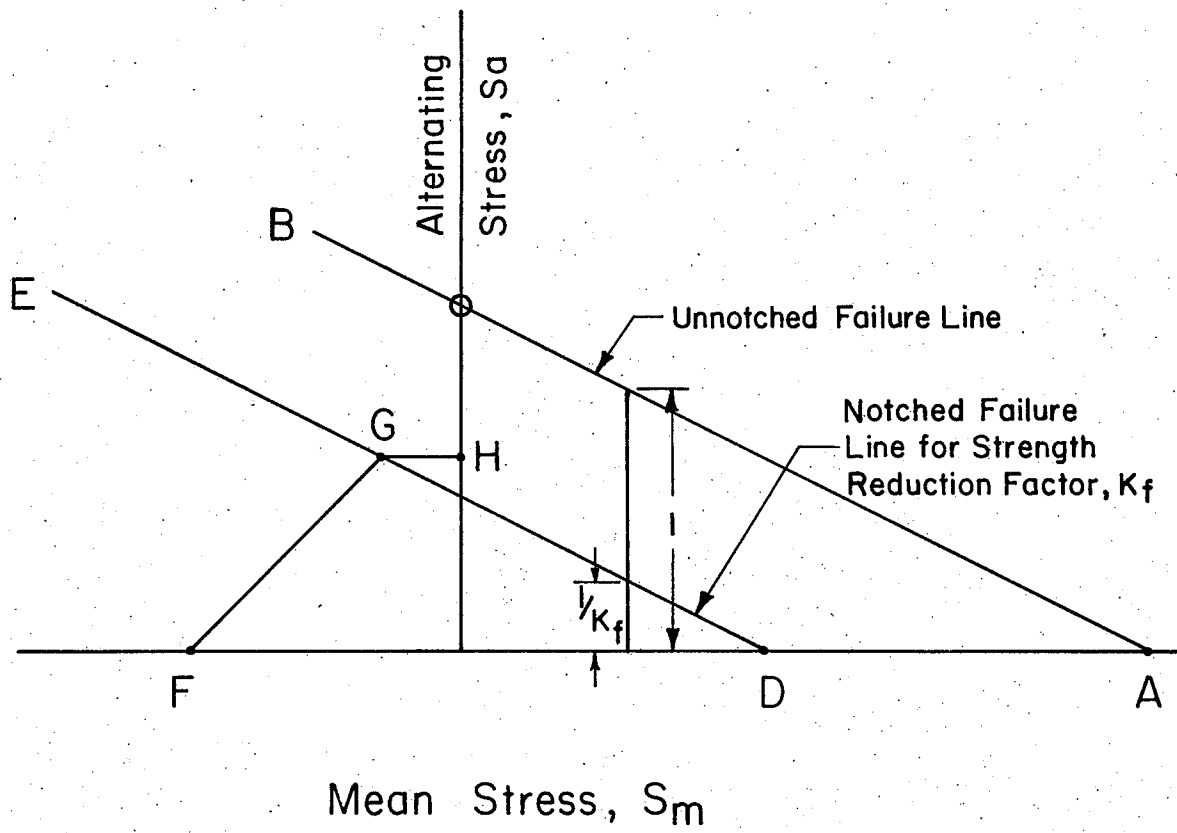


Figure 5.4. Graphical Method of Fatigue Strength Prediction

Employing the Goodman lines in Figure 3.5 and the experimentally determined fatigue strength reduction factors in Figure 5.5, the 'notched' Goodman lines in Figure 5.6 are drawn with one consideration. The static strength of a notched component is equivalent to the ultimate tensile strength of the material. Therefore instead of permitting the 'notched' Goodman lines from intersecting the mean stress axis at a value below the latter strength, the alternating stresses were reduced exponentially from the line MN according to the relation

$$S_a = e^{CS_m} + Z \text{ ksi.} \quad (5.2)$$

where

C and Z are constants for the particular 'notched' Goodman line such that all the lines intersected the mean stress axis at the ultimate tensile strength of the material. The results of Fisher and Yeomans (7) plotted in Figure 5.7 add support to this. Selecting the measured residual stress of -26.5 ksi. (14) to be the effective residual stress in the region of the hole, the method yields a dimpled loaded-hole fatigue strength of approximately  $9.25 \pm 9.25$  ksi. at  $10^6$  cycles to failure as compared to  $9.05 \pm 9.05$  ksi. experimentally.

(b) Dimpled; Interference-Fit Pin

Two additions to the previous method are now introduced for the case of an interference-fit pin. Firstly, an initial interference fit is considered to create a shift along the mean stress axis by an amount equal to the nominal interference hoop stress in the region of the hole boundary.

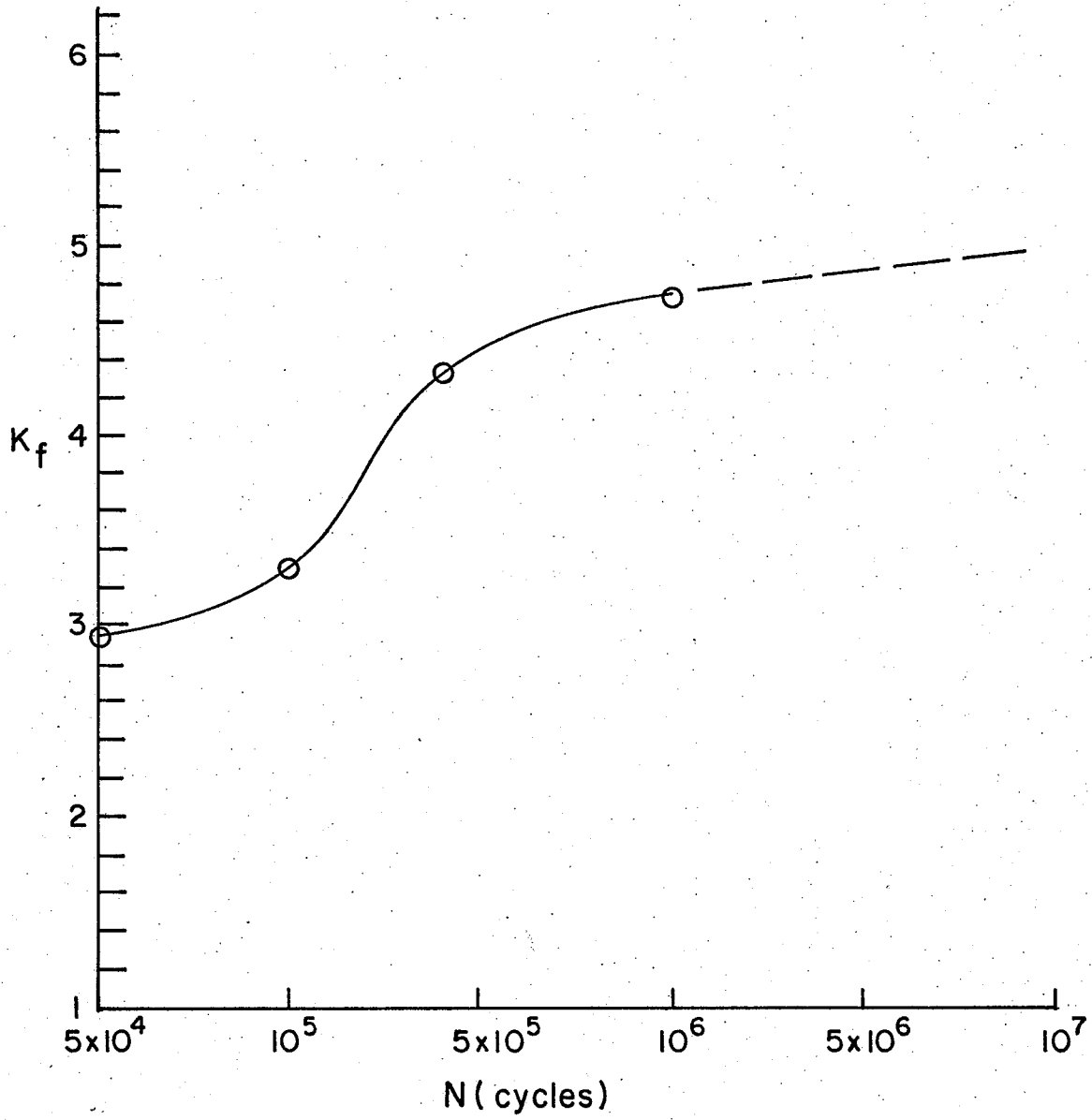


Figure 5.5. Variation of the Present Experimental Fatigue Strength Reduction Factor,  $K_f$ , With Life

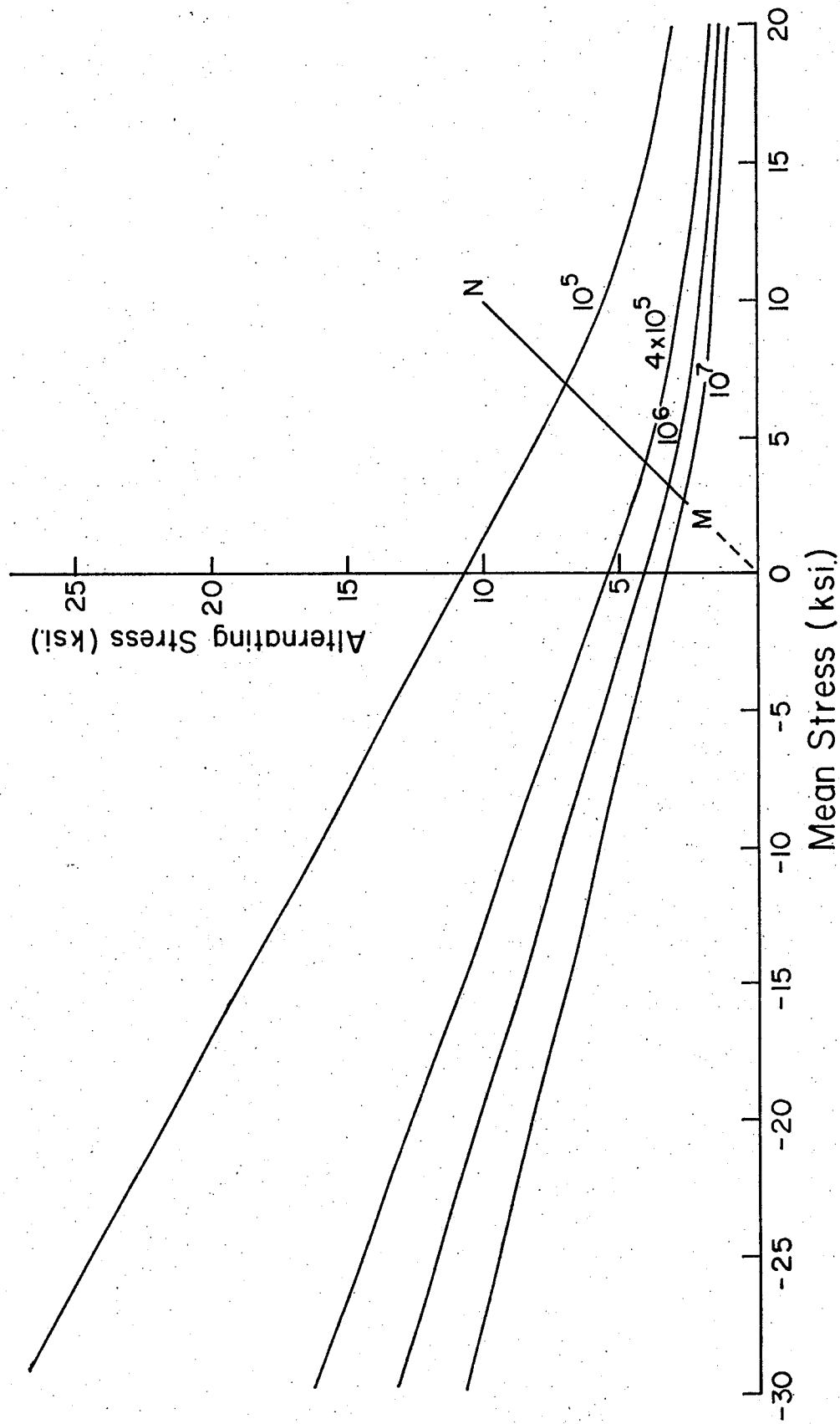


Figure 5.6 'Notched' Failure Lines for the Present Investigation

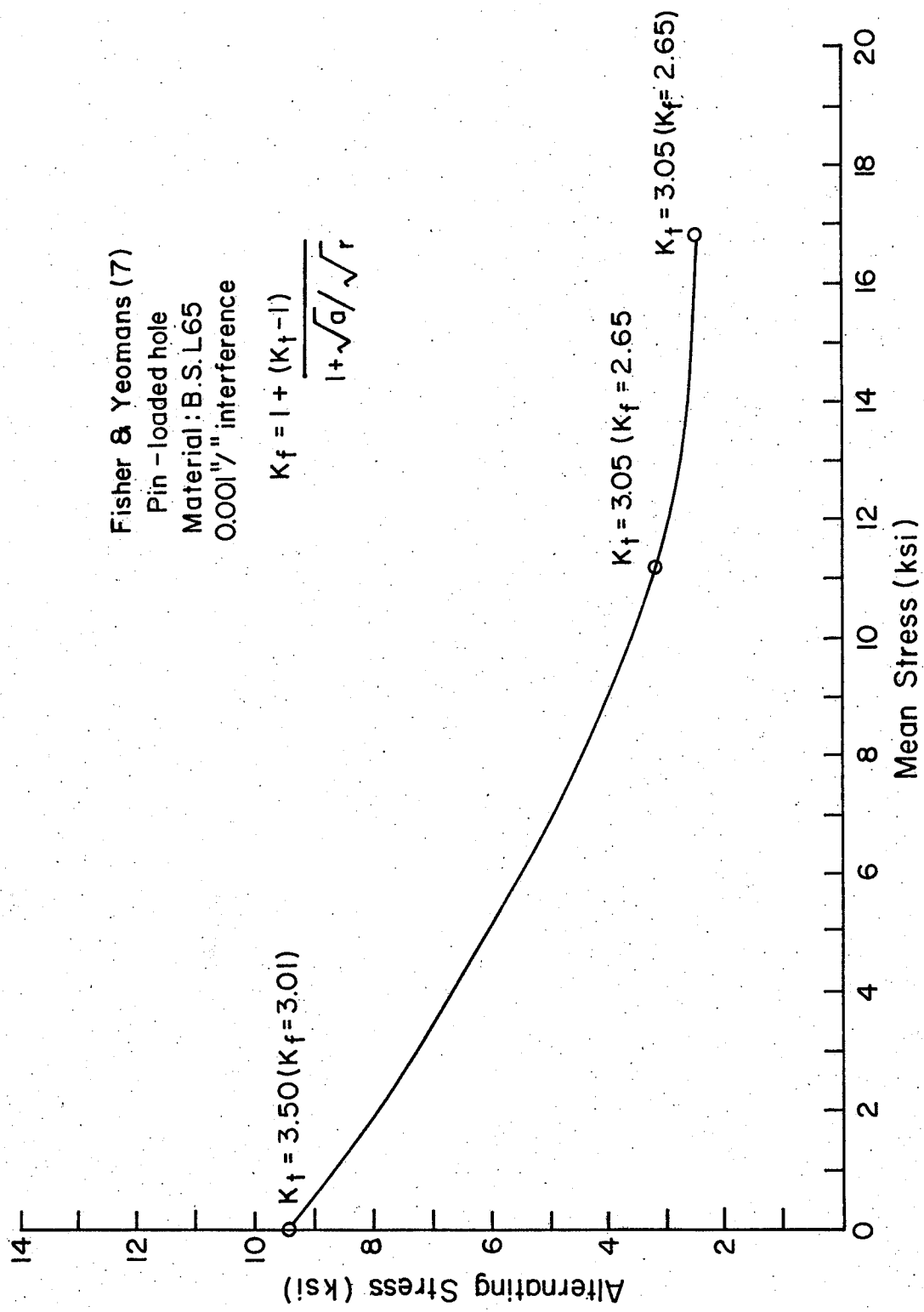


Figure 5.7 'Notched' Failure Line for  $10^6$  Cycles to Failure (7)



In order to obtain a good estimate for the latter, an interference hoop stress profile for the minimum net section is constructed according to Lamé thick cylinder theory. The profile in Figure 5.8 is obtained for the present specimen dimensions. Considering the entire cross section, interference produces a nominal hoop stress of approximately 19 percent of the hole boundary hoop stress. For the plate material near the hole boundary in which dimpling produces residual compressive stresses ranging from about -26.5 to -23.5 ksi., a nominal interference hoop stress of approximately 46 percent of the hole boundary hoop stress exists. The latter is chosen to represent the shift along the mean stress axis due to an initial interference fit thereby leading to a better estimate of the net residual hoop stress in the region of the hole prior to fatigue loading. Concerning the second addition, the slope  $S_a/S_m$  of the loading line is determined from the curve of Figure 5.9 constructed from the hole boundary hoop stresses of the minimum net section in Figure 2.1. Note that now the stress ratio  $S_a/S_m$  is not identical to the load ratio  $P_a/P_m$  in the presence of an interference fit. By employing the dimensionless stress ratios in Figure 5.9,  $S_a/S_m$  may be evaluated for any loaded hole  $K_t$  or  $K_f$  value. The stresses are once again calculated as elastic stresses. Given  $S_{INT}$ ,  $K_f$ , and  $S_{NOM}$ ,  $S_a/S_m$  may be found as outlined below. Given  $S_{INT}$  and  $S_{NOM}$ , a value for  $K_f$  is chosen from Figure 5.5 on the basis of an expected life. Then

$$\frac{S_{INT}}{K_f S_{NOM}} = A \quad (5.3)$$

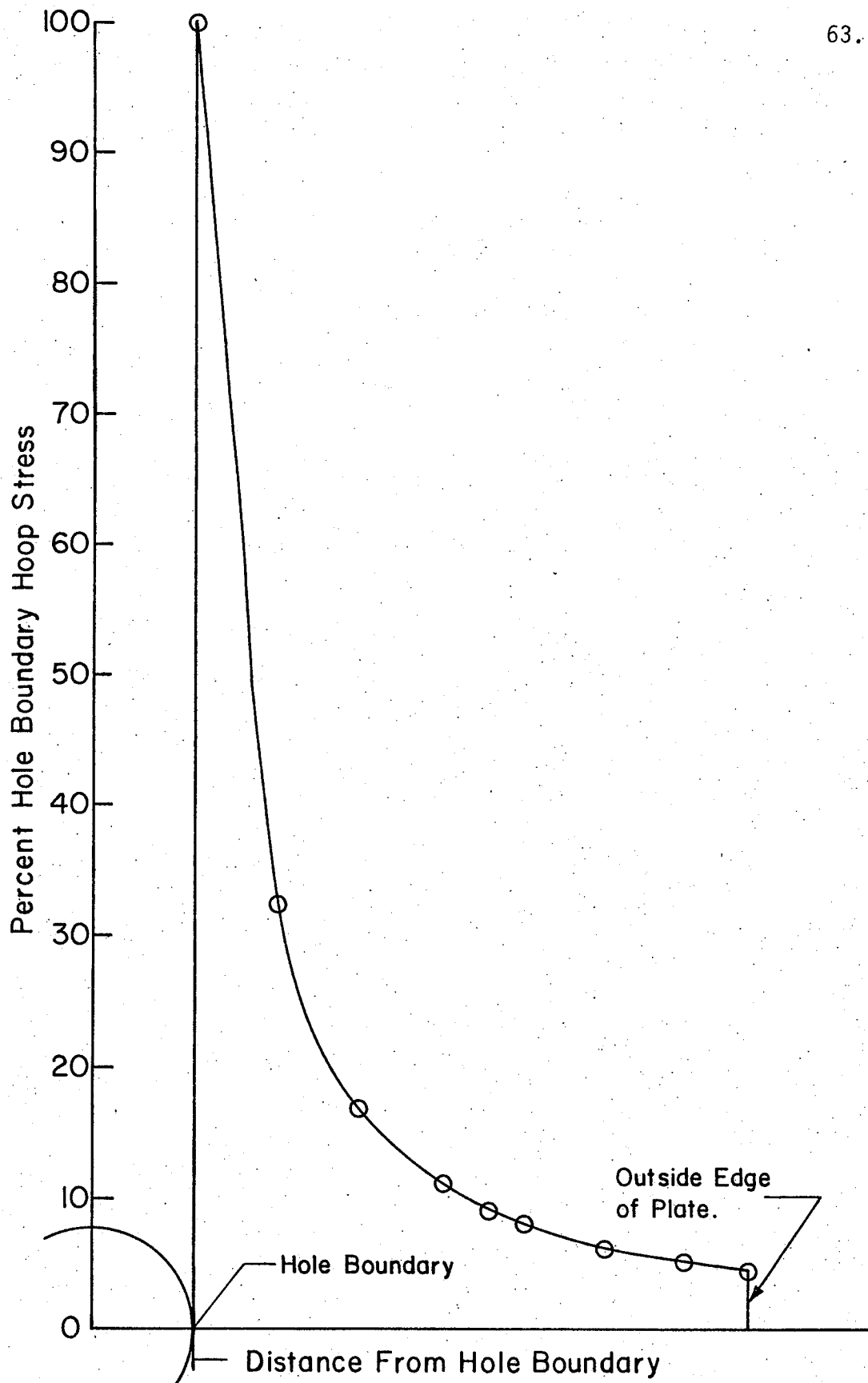


Figure 5.8 Interference Hoop Stress Profile Over the Minimum Net Section for the Present Investigation

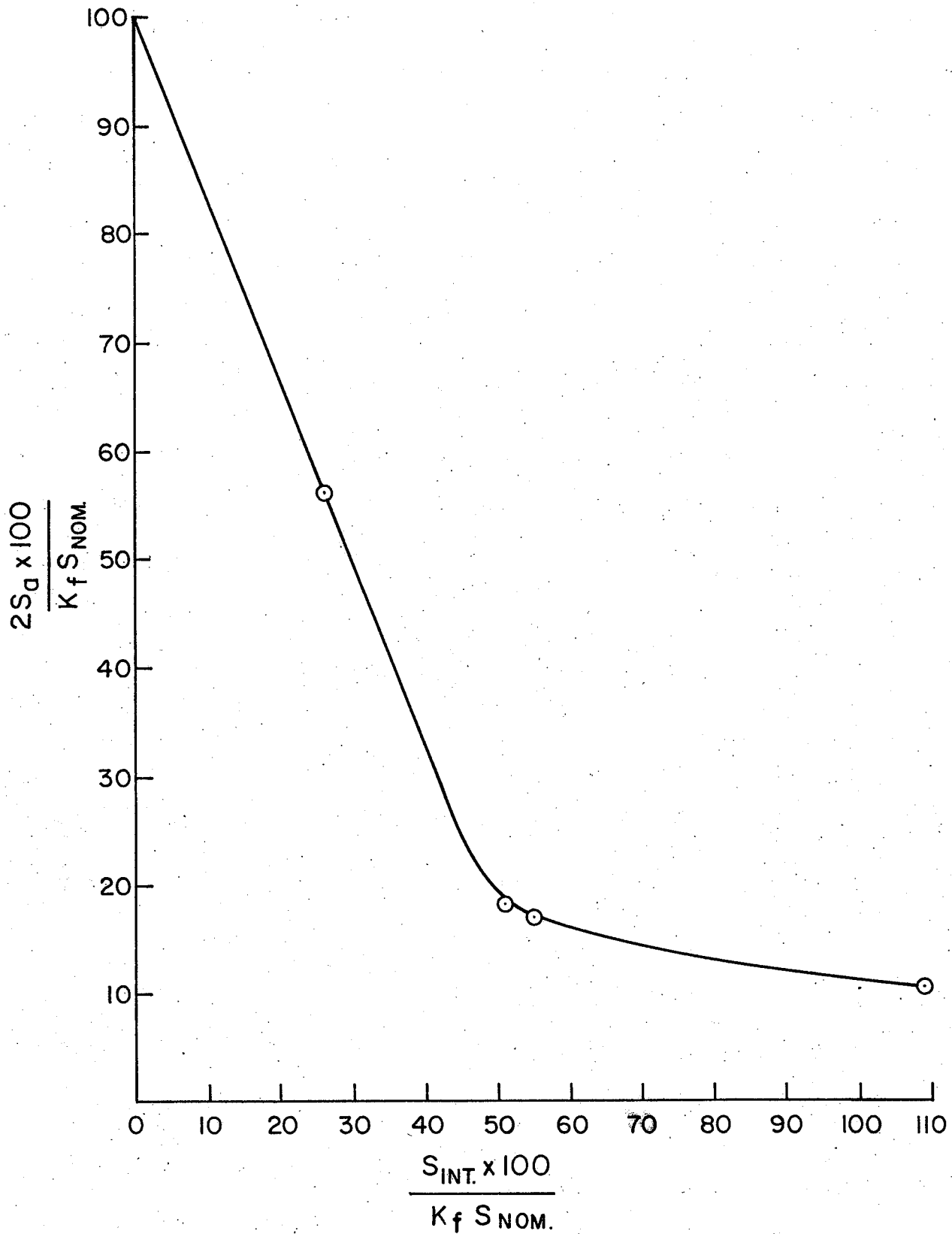


Figure 5.9 Variation of  $S_a$  with Interference for a Pin-Loaded Hole Subjected to Zero-to-Tension Loading

and

$$\frac{2S_a}{K_f S_{NOM}} = B \quad \text{from Figure 5.9.} \quad (5.4)$$

Now

$$\frac{S_a}{S_m} = \frac{S_a}{S_a + S_{INT}} \quad (5.5)$$

Putting (5.3) and (5.4) into (5.5)

$$\frac{S_a}{S_m} = \frac{B}{2A + B} \quad (5.6)$$

A line of slope corresponding to the ratio of  $S_a/S_m$  is drawn on Figure 5.6 from the new loading origin on the mean stress axis equal to

$$-26.5 + 0.46S_{INT} \text{ ksi.}$$

The line is drawn to a height corresponding to

$$S_{eNOM} = S_a/K_f = B/2 S_{NOM} \quad (5.7)$$

The point where the line terminates determines the life for the given nominal applied stress. If the obtained life is sufficiently different from the expected life,  $K_f$  is adjusted for another trial.

Applying this technique to the  $9 \pm 9$  and  $10 \pm 10$  ksi. nominal applied stress levels where hole elongation is small and failures occur at the hole boundary at or near the minimum net section, the predicted values of fatigue life are entered in Table 5.4 in comparison to the values obtained experimentally. Close agreement between the two was achieved. Taking an interference of 0.008 inch per inch, the technique

TABLE 5.4

Comparison of Predicted and Actual Fatigue Lives  
for Present Investigation

$S_{NOM}$ (ksi.)	Interference (inch/inch)	Predicted Fatigue Life (cycles)	Actual Median Fatigue Life (cycles)
9 $\pm$ 9	0.006	$>10^7$	$1.6 \times 10^6$
9 $\pm$ 9	0.008	$>10^7$	$4.0 \times 10^6$
10 $\pm$ 10	0.006	$6 \times 10^6$	$7 \times 10^5$ *
10 $\pm$ 10	0.008	$2 \times 10^6$	$10^6$
10 $\pm$ 10	0.010	$5 \times 10^5$	$2 \times 10^6$

\* Interpolated

predicted a fatigue strength between  $9 \pm 9$  and  $10 \pm 10$  ksi. at about  $4 \times 10^6$  cycles to failure as compared to  $9 \pm 9$  ksi, found experimentally.

## CHAPTER 6

## SUMMARY AND CONCLUSIONS

6.1 Summary

The effect of interference on the fatigue strength of a dimpled loaded hole has been studied. The concept of an optimum interference fit for a given loading of a component was examined by the application of various degrees of interference for each stress level concerned.

6.2 Conclusions

The following conclusions can be drawn:

1. Optimum interference enhances the dimpled, loaded hole fatigue strength of 2024-T3 alclad, aluminum-alloy sheet under zero-to-tension loading.
2. For increasing loads, optimum fatigue strength improvement requires increasing interference.
3. Fatigue strength improvements due to dimpling are reproducible.
4. The dimpled loaded-hole fatigue strength and/or life of 2024-T3 alclad aluminum alloy sheet may be reasonably predicted by the aforesaid technique for the cases of a push-fit and interference-fit pin when considering nominal applied stresses where hole elongation for the former case is small and failures occur at the hole boundary at or near the minimum net section.

### 6.3 Suggestions for Further Study

1. The interference-optimization testing for dimpled specimens at maximum nominal stress levels of 18, 20 and 22 ksi. could be completed.
2. Similarly, interference-optimization testing could be extended to undimpled specimens.
3. Dimpling could be extended to other metals.
4. The effect of mean and alternating stresses on the fatigue strength of unloaded and/or loaded holes could be investigated in order to better envision the shape of the notched-specimen curve on  $S_a$ - $S_m$  coordinates.



BIBLIOGRAPHY

1. Jessop, H. T., Snell, C. and Holister, G. S., "Photoelastic Investigation on Plates with Single Interference-Fit Pins with Load Applied (a) to Pin only, and (b) to Pin and Plate Simultaneously," The Aeronautical Quarterly, Vol. IX, May, 1958, p. 147.
2. Ligenza, S. J., "Cyclic Stress Reduction Within Pin-Loaded Lugs Resulting from Optimum Interference Fits," Experimental Mechanics, Soc. Experimental Stress Analysis, Vol. 3, No. 1, P. 21, Jan. 1963.
3. Lambert, T. H. and Brailey, R. J., "The Influence of the Coefficient of Friction on the Elastic Stress Concentration Factor for a Pin-Jointed Connection," The Aeronautical Quarterly, 1962.
4. Fisher, W. A. P., and Winkworth, W. J., "Improvements of the Fatigue Strength of Joints by the Use of Interference Fits," RAE Structure Rpt. 127, May, 1952.
5. Fisher, W. A. P., and Winkworth, W. J., "Improvement in the Fatigue Strength of Joints by the Use of Interference Fits," ARC R & M 2874, 1955.
6. Schijve, J., Broek, D. and Jacobs, F. A., "Fatigue Tests on Aluminum Alloy Lugs with Special Reference to Fretting," NAA Rsch. Inst. Rpt. No. TNM 2103, Amsterdam, March, 1962.
7. Fisher, W. A. P. and Yeomans, H., "Fatigue Strength of Aluminum Alloy Lugs With and Without Interference Pins," Unpubl. MOA Rpt., Nov. 1956.
8. Hartman, A. and Jacobs, F. A., "Effects of Various Fits on the Fatigue Strength of Pin-Hole Joints," NLL Rpt. M 1946, April 1954; ARC Rpt. 17371, Struct. 1772.
9. Low, A. C., "The Fatigue Strength of Pin-Jointed Connections in Aluminum Alloy BS L65," Proc., Institution of Mechanical Engineers, Vol. 172, No. 27, 1958, pp. 821-38.
10. Smith, C. R., "Design Applications for Improving Fatigue Resistance of Airplane Structures," Proc., American Society for Testing and Materials, Vol. 60, 1960, pp. 589-601.
11. Smith, C. R., "Tapered Bolts - Their Influence on Fatigue of Airplane Structures," Convair Rpt. No. ZR-659-053, May, 1960.

12. Mittenbergs, A. A. and Beall, L. G. Jr., "Effects of Pin-Interference and Bolt Torque on Fatigue Strength of Lug Joints," Proc., American Society for Testing and Materials, Vol. 63, 1963, pp. 671-683.
13. White, D. J., "Fatigue Strength of Small Pinned Connections made from Alloy Steel FV 520 B," Proc., Institution of Mechanical Engineers, Vol. 182, 1967-68, pp. 615-630.
14. Shewchuk, J. and Roberts, F. A., "Increasing the Fatigue Strength of Loaded Holes by Dimpling," Trans., ASME, Jnl. Engrg. Materials and Technology, 96(3), July 1974, pp. 222-26.
15. Shewchuk, J., "Decreasing the Fatigue Strength Reduction Factor by Dimpling," Journal of Testing and Evaluation, JTEVA, Sept., 1974, Vol. 2, No. 5, pp. 425-28.
16. Heywood, R. B., "Designing Against Fatigue," Chapman and Hall Ltd., 1962, pp. 168-201.
17. Metals Handbook, 8th Ed., American Society for Metals, Cleveland, 1964, Vol. 1, p. 940.
18. Juvinal, R. C., "Stress, Strain, and Strength," McGraw-Hill Book Company, 1967, pp. 193-341.
19. Lambert, T. H., "Elastic Stresses Due to an Interference-Fit Pin in a Rectangular Plate of Finite Width," Journal of Mechanical Engineering Science, Vol. 3, 1961, p. 236.